Distance Ladder and H_0

Classical Cosmology

To understand what universe we live in, we need to determine observationally the following numbers:

1. The Hubble constant, H_0

   $\Longrightarrow$ Requires distance measurements.
2. The current density parameter, Ω_0

   $\Longrightarrow$ Requires measurement of the mass density.
3. The cosmological constant, Λ

   $\Longrightarrow$ Requires acceleration measurements.
4. The age of the universe, t_0, for consistency checks

   $\Longrightarrow$ Requires age measurements.

The determination of these numbers is the realm of classical cosmology.

First part: Distance determination and H_0!

Introduction, I

Distances are required for determination of H_0.

$\Longrightarrow$ Need to measure distances out to $\sim$200 Mpc to obtain reliable values.

To get this far: cosmological distance ladder.

1. Trigonometric Parallax and Moving Cluster
2. Main Sequence Fitting
3. RR Lyr
4. Baade-Wesselink
5. Cepheids
6. (Light echos)
7. Brightest Stars
8. Type Ia Supernovae
9. Tully-Fisher
10. D_n-σ for ellipticals
11. Brightest Cluster Galaxies
12. Gravitational Lenses

Still the best reference on this subject is ROWAN-ROBINSON, M., 1985, The Cosmological Distance Ladder, New York: Freeman.

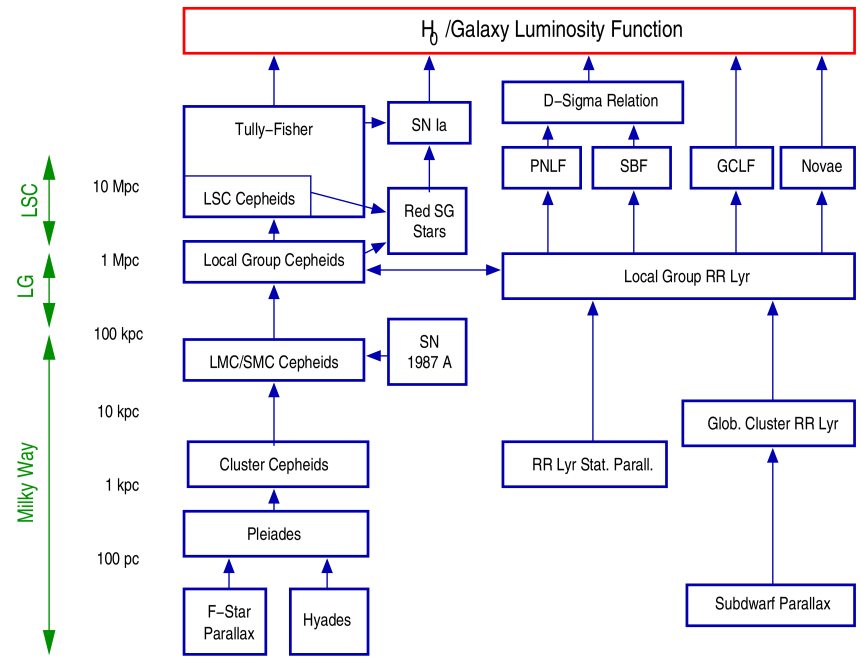

(after Jacoby et al., 1992, Fig. 1)

Units

Basic unit of length in astronomy: Astronomical Unit (AU).

Colloquial Definition: 1 AU $=$ mean distance Earth–Sun.

Measurement: (Venus) radar ranging, interplanetary satellite positions, χ^2 minimization of N-body simulations of solar system

1 AU $\sim$ 149.6 $\times$ 10^6 km

In the astronomical system of units (IAU 1976), the AU is defined via Gaussian gravitational constant (k), where the acceleration

$$\ddot{\boldsymbol{r}} = -\frac{k^2(1+m)\boldsymbol{r}}{r^3}$$

where k := 0.01720209895, leading to $a_\oplus$ = 1.00000105726665, and 1 AU=1.4959787066 $\times$ 10^{11} m (Seidelmann, 1992).

Reason for this definition: k much better known than G.

(2006 CODATA: $G = 6.67428(67) \times 10^{-11}\,\mathrm{m}^3\,\mathrm{kg}^{-1}\,\mathrm{s}^{-2}$, so only known to 4 significant digits)

Trigonometric Parallax, I

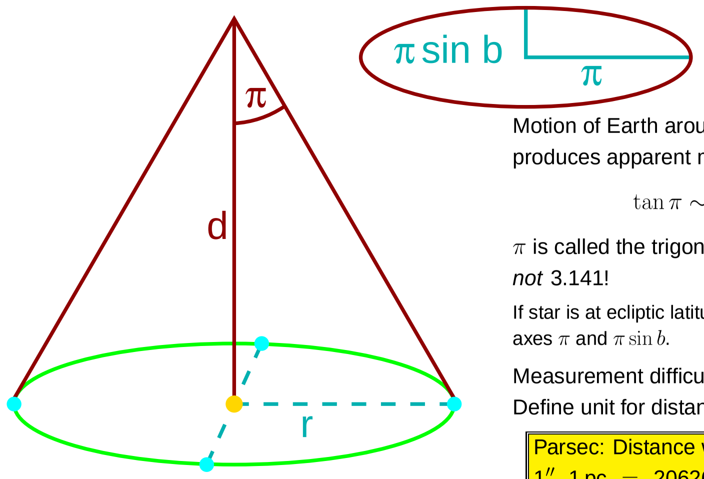

Motion of Earth around Sun $\Longrightarrow$ Parallax produces apparent motion by amount

$$\tan\pi \sim \pi = r_\oplus/d \qquad (9.1)$$

π is called the trigonometric parallax, and *not* 3.141!

If star is at ecliptic latitude b, then ellipse with axes π and $\pi\sin b$.

Measurement difficult: $\pi \lesssim 0.76''$ (α Cen).

Define unit for distance:

Parsec: Distance where 1 AU has π = $1''$. 1 pc = 206265 AU = 3.08 $\times$ 10^{18} cm = 3.26 ly

after Rowan-Robinson (1985, Fig. 2.1)

Trigonometric Parallax, II

Best measurements to date: Hipparcos satellite (1989–1993)

- systematic error of position: $\sim$0.5 mas for stars brighter 9 mag
- effective distance limit: 1 kpc
- standard error of proper motion: $\sim$1 mas yr^{-1}
- broad band photometry
- narrow band: B $-$ V, V $-$ J
- magnitude limit: 12 mag
- complete to mag: 7.3–9.0

Results available at `http://www.rssd.esa.int/index.php?project=HIPPA`

Hipparcos catalogue: 118 218 objects with milliarcsecond precision.

Tycho catalogue: 2 539 913 stars with 20–30 mas precision, two-band photometry (99% complete down to 11 mag)

Revised Hipparcos calibration: see van Leeuwen (2007).

GAIA (ESA mission, to be launched 2011 Dec on Soyuz from Kourou):

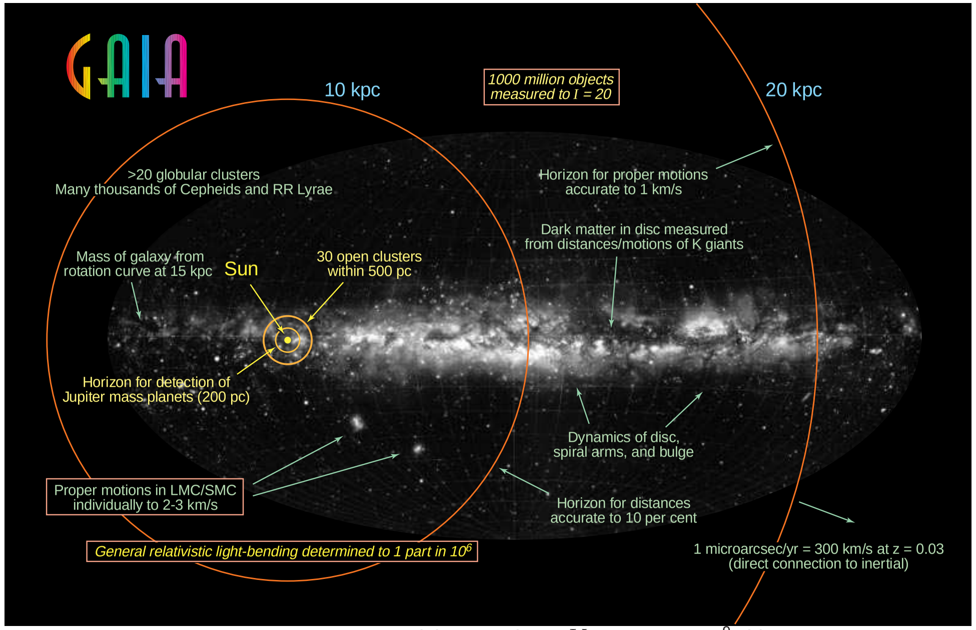

GAIA: $\sim 4\mu$arcsec precision, 4 color to $V = 20$ mag, 10^9 objects.

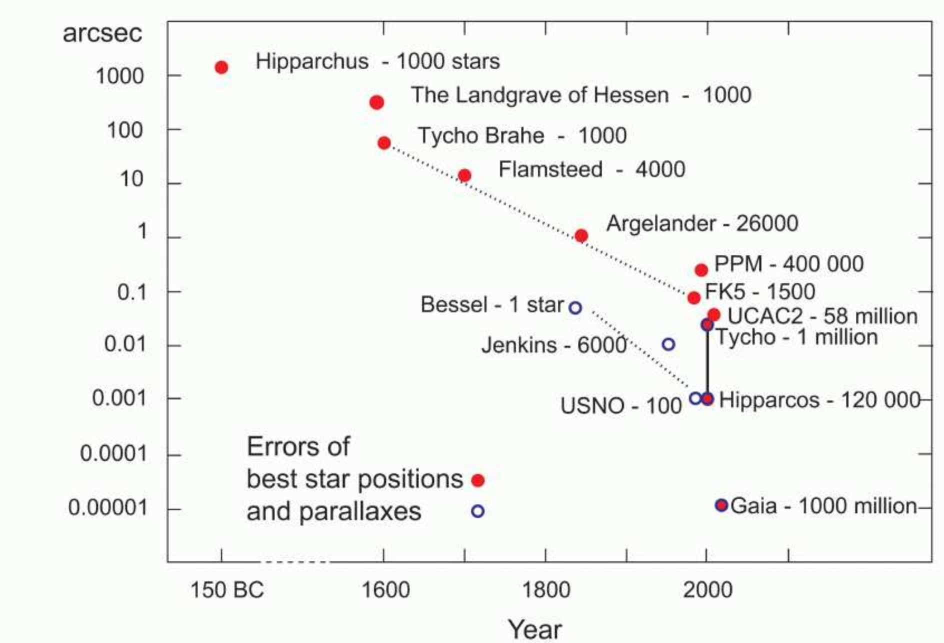

ESA/M. Perryman

Development of the precision of astronomical position measurements

© Till Credner

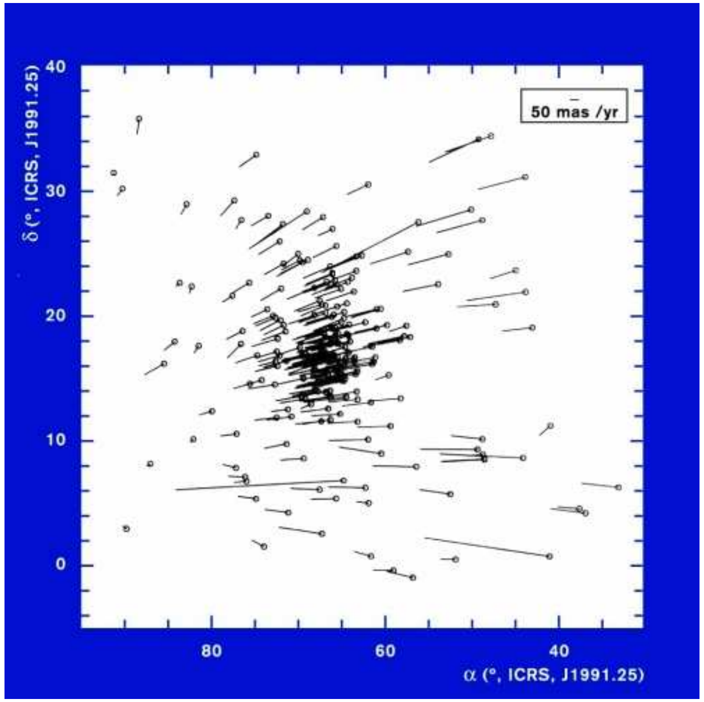

Source: ESA

Moving Cluster

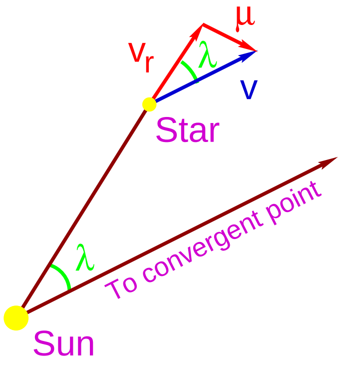

Perspective effect of spatial motion towards convergent point:

$$\tan\lambda = \frac{v_\mathrm{t}}{v_\mathrm{r}} = \frac{\mu d}{v_\mathrm{r}} \tag{9.2}$$

or

$$\frac{d}{1\,\mathrm{pc}} = \frac{v_\mathrm{r}/(1\,\mathrm{km/s})\tan\lambda}{4.74\,\mu/(1''/\mathrm{a})} \tag{9.3}$$

Problem: determination of convergent point

Less error prone: moving cluster method = rate of variation of angular diameter of cluster:

$$\dot{\theta} d = \theta v_\mathrm{r} \tag{9.4}$$

Observation of proper motions gives

$$\frac{\dot{\theta}}{\theta} = \frac{\mathrm{d}\mu_\alpha}{\mathrm{d}\alpha} = \frac{\mathrm{d}\mu_\delta}{\mathrm{d}\delta} \tag{9.5}$$

where $\mu_{\alpha,\delta}$ proper motion in α and δ. Therefore, from Eq. (9.4),

$$d = v_\mathrm{r}\frac{\dot{\theta}}{\theta} \tag{9.6}$$

Moving Cluster

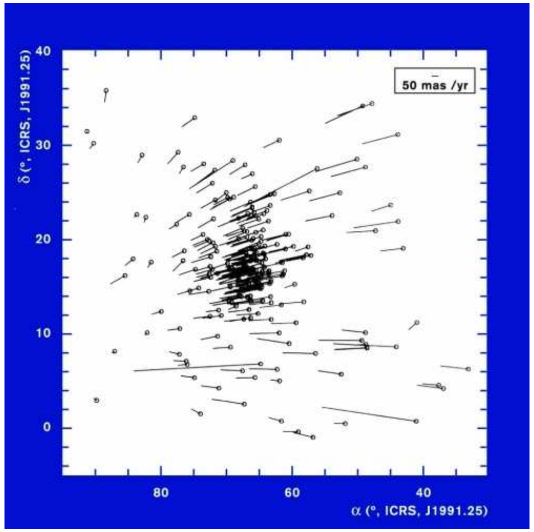

Source: ESA

Application: Distance to Hyades. Tip of "arrow": Position of stars in 100000 years.

Hanson (1980) finds from this a distance of 46 pc

However: *Hipparcos:* geometric distance to Hyades is $d = 46.34 \pm 0.27$ pc from parallax measurements.

$\Longrightarrow$ Moving cluster method only of historic interest.

Interlude

Parallax and Moving Cluster: geometrical methods.

All other methods (exception: light echoes): standard candles.

Requirements for standard candles (Mould, Kennicutt, Jr. & Freedman, 2000):

1. Physical basis should be understood.
2. Parameters should be measurable objectively.
3. No corrections ("fudges") required.
4. Small intrinsic scatter ($\Longrightarrow$ requiring small number of measurements!).
5. Wide dynamic range in distance.

Magnitudes

Assuming isotropic emission, distance and luminosity are related ("inverse square law") $\Longrightarrow$ luminosity distance:

$$F = \frac{L}{4\pi d_{\mathrm{L}}^2} \tag{9.7}$$

where F is the measured flux (erg cm^{-2} s^{-1}) and L the luminosity (erg s^{-1}).

Definition also true for flux densities, I_ν (erg cm^{-2} s^{-1} Å^{-1}).

The magnitude is defined by

$$m = A - 2.5 \log_{10} F \tag{9.8}$$

where A is a constant used to define the zero point (defined by $m = 0$ mag for Vega).

For a filter with transmission function ϕ_ν,

$$m_i = A_i - 2.5 \log \int \phi_\nu F_\nu \, \mathrm{d}\nu \tag{9.9}$$

where, e.g., $i =$ U, B, V.

Magnitudes

To enable comparison of luminosities: define

absolute magnitude $M =$ magnitude at distance 10 pc

Thus, since $m = A - 2.5 \log(L/4\pi d^2)$,

$$M = m - 5 \log\left(\frac{d_{\mathrm{L}}}{10\,\mathrm{pc}}\right) \tag{9.10}$$

The difference $m - M$ is called the distance modulus, μ_0:

$$\mu_0 = \mathrm{DM} = m - M = 5 \log\left(\frac{d_{\mathrm{L}}}{10\,\mathrm{pc}}\right) \tag{9.11}$$

Often, distances are given in terms of $m - M$, and not in pc.

DM [mag]	3	5	10	15	20	25	30
d	40 pc	100 pc	1 kpc	10 kpc	100 kpc	1 Mpc	10 Mpc

Main Sequence Fitting, I

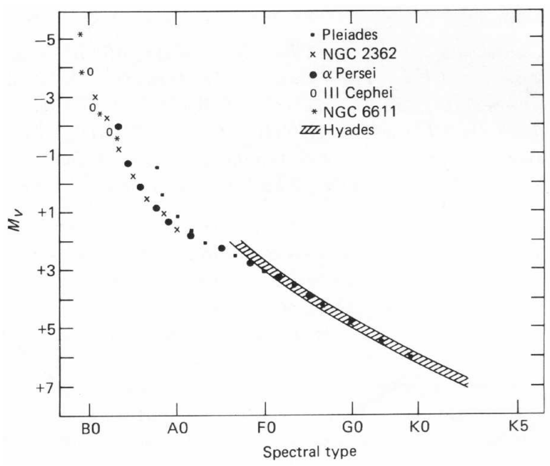

after Rowan-Robinson (1985, Fig. 2.11)

All open clusters are comparably young

$\Longrightarrow$ Hertzsprung Russell Diagram (HRD) dominated by Zero Age Main Sequence (ZAMS).

$\Longrightarrow$ Measure HRD (or Color Magnitude Diagram; CMD), shift magnitude scale until main sequence aligns

$\Longrightarrow$ distance modulus.

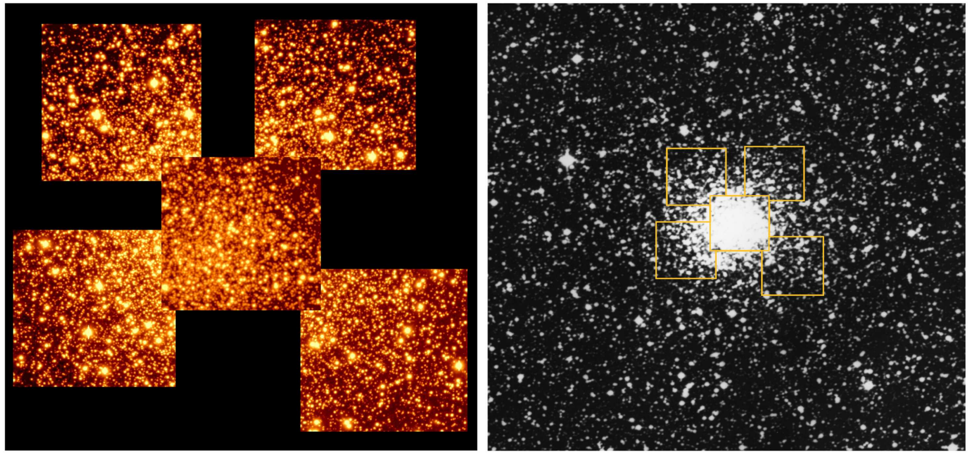

Globular Cluster NGC 6712

ESO PR Photo 06a/99 (18 February 1999)

© European Southern Observatory

Main Sequence Fitting, II

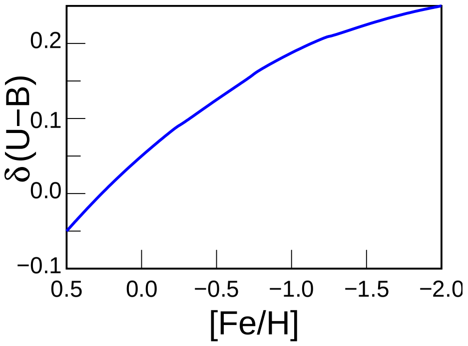

(after Rowan-Robinson, 1985, Fig. 2.12)

Caveats:

1. Location of ZAMS more age dependent than expected (van Leeuwen, 1999).
2. interstellar extinction
   $\Longrightarrow$ $\mu_0 = \mu_\mathrm{V} - A_\mathrm{V}$, where μ_V, A_V DM/extinction measured in V-band.
3. metals: line blanketing (change in stellar continuum due to metal absorption lines, see figure)
   $\Longrightarrow$ Changes color
   $\Longrightarrow$ horizontal shift in CMD.

van den Bergh (1977): $Z_\text{Hyades} \sim 1.6 Z_\odot$, while other open clusters have solar metallicity $\Longrightarrow$ Cepheid DM were overestimated by 0.15 mag.

4. identification of unevolved stars crucial (evolution to larger magnitudes on MS during stellar life).

Currently: distances to ∼200 open clusters known (Fenkart & Binggeli, 1979), limit ∼7 kpc.

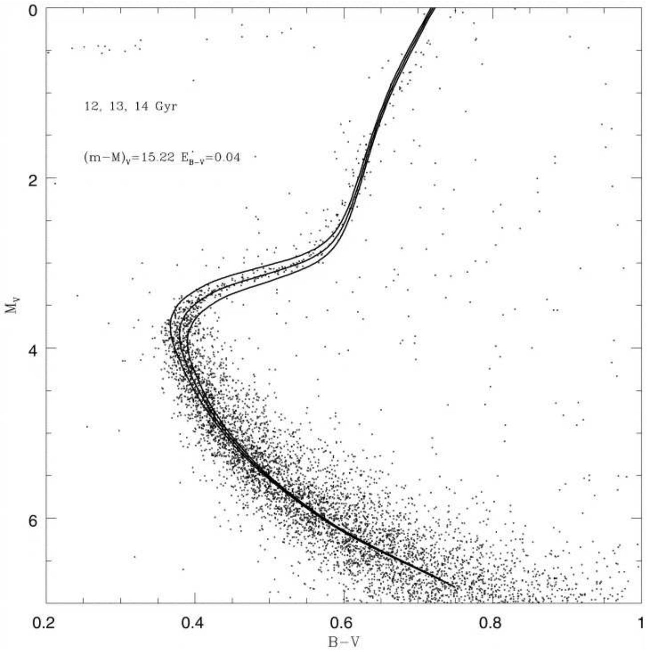

(M68, Straniero, Chieffi & Limongi, 1997, Fig. 11)

Globular clusters: HRD different from open clusters:

- population II
  $\Longrightarrow Z \ll Z_\odot$
- evolved

Use theoretical HRDs (isochrones) to obtain distance.

For distant clusters: MS unobservable

$\Longrightarrow$ position of horizontal branch.

Baade-Wesselink

Basic principle (Baade, 1926): Assume black body

$\Longrightarrow$ Use color/spectrum to get kT_{eff}

$\Longrightarrow$ Emitted intensity is Planckian, B_ν

$\Longrightarrow$ Observed Intensity is $I_\nu \propto \pi R_*^2 \cdot B_\nu$.

Radius from integrating velocity profile of spectral lines:

$$R_2 - R_1 = p \int_1^2 v \, \mathrm{d}t \tag{9.12}$$

(p: projection factor between velocity vector and line of sight).

Wesselink (1947): Determine brightness for times of same color

$\Longrightarrow$ rather independent of knowledge of stellar spectrum (deviations from B_ν).

Stars: Calibration using interferometric diameters of nearby giants.

Baade-Wesselink works for pulsating stars such as RR Lyr, Cepheids, Miras, and expanding supernova remnants.

RR Lyr

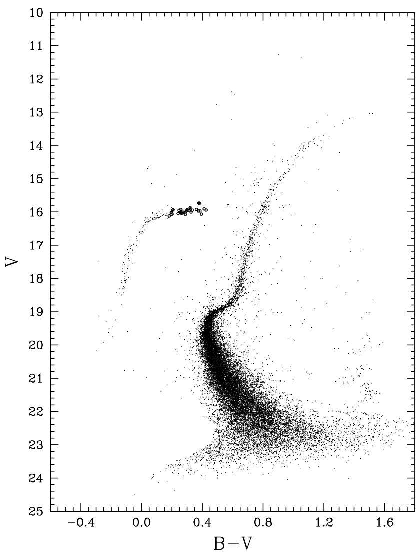

RR Lyrae variables: Stars crossing instability strip in HRD

$\Longrightarrow$ Variability ($P \sim 0.2 \ldots 1\,\mathrm{d}$)

$\Longrightarrow$ RR Lyr gap (change in color!).

Absolute magnitude of RR Lyr gap:

$M_{\mathrm{V}} = 0.6$, $M_{\mathrm{B}} = 0.8\,\mathrm{mag}$, i.e.,

$L_{\mathrm{RR}} \sim 50\,L_\odot$.

M determined from ZAMS fitting, statistical parallax, and Baade-Wesselink method.

M2: Lee & Carney (1999, Fig. 2)

RR Lyr

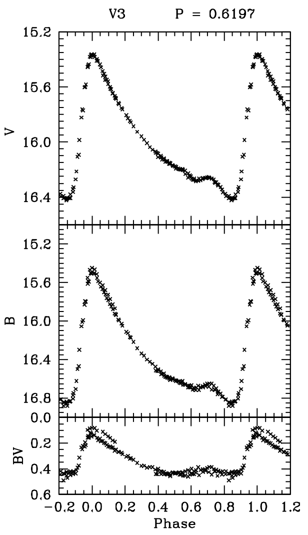

Lightcurve shows characteristic color variations over pulsation (temperature change!), and a fast rise, slow decay behavior.

RR Lyr in GCs show bimodal number distribution due to a metallicity effect:

- RRab with $P > 0.5\,\mathrm{d}$ and most probable period of $P_{\mathrm{ab}} \sim 0.7\,\mathrm{d}$, and
- RRc, with $P < 0.5\,\mathrm{d}$ and $P_{\mathrm{c}} \sim 0.3\,\mathrm{d}$.

M is larger for higher Z, i.e., metal-rich RR Lyr are *fainter*

$\Longrightarrow$ difference in RR Lyr from population I and II.

RR Lyr work out to LMC and other dwarf galaxies of local group, however, used mainly for globular clusters.

(Lee & Carney, 1999, Fig. 5)

Interlude

Previous methods: Selection of methods for distances within Milky Way (and Magellanic Clouds): Basis for extragalactic distance scale.

Primary extragalactic distance indicators: Distance can be calibrated from observations *within* milky way or from theoretical grounds.

Primary indicators usually work within our neighborhood (i.e., out to Virgo cluster at 15–20 Mpc).

Examples: Cepheids, light echos,. . .

Secondary extragalactic distance indicators: Distance calibrated from primary distance indicators.

Examples: Type Ia SNe, methods based on integral galaxy properties.

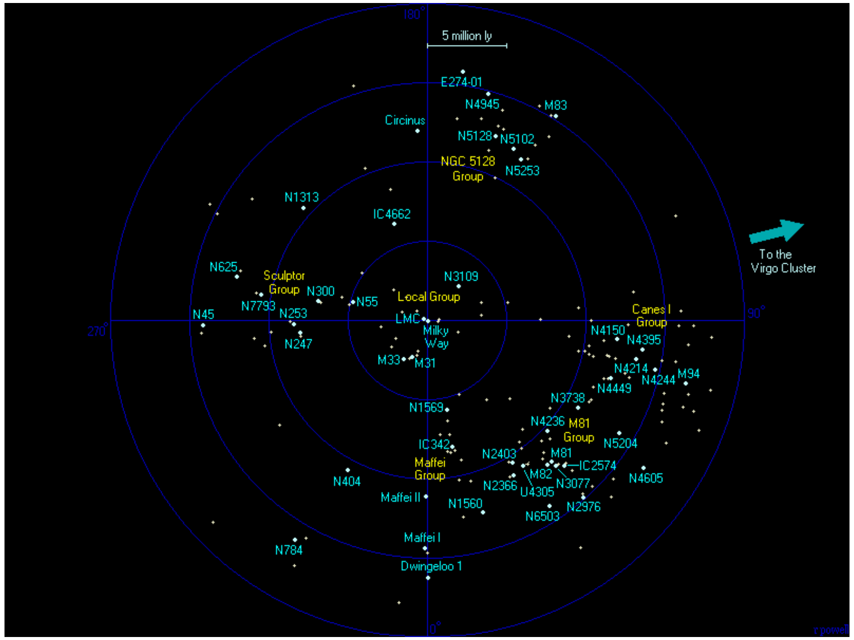

source: `http://www.atlasoftheuniverse.com/galgrps.html`

700 kpc: M31 (Andromeda)

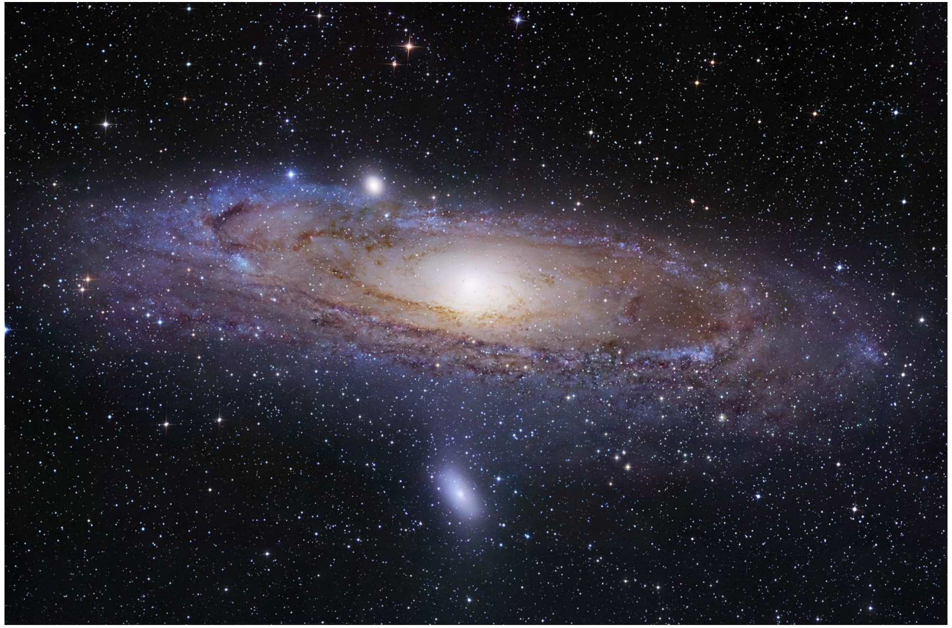

Robert Gendler
the largest astronomical picture ever taken, 21904 × 14454 pixels

To get a feel for the distances in our “neighborhood”:

50 kpc: LMC, SMC, some other dwarf galaxies

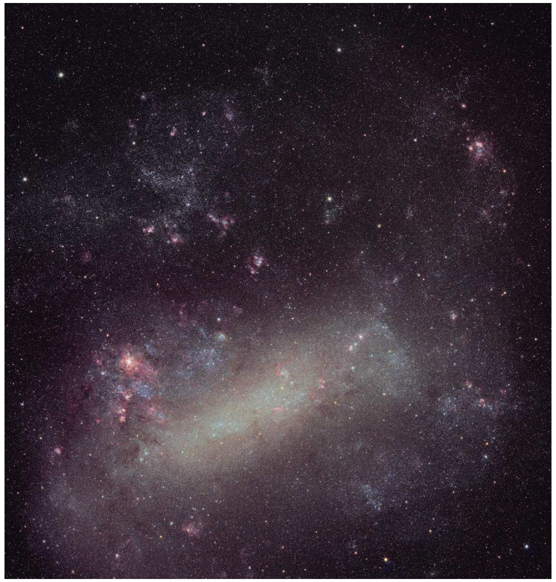

Loke Kun Tan

2–3 Mpc: Sculptor and M81 group

(groups similar to local group: a few large spirals, plus smaller stuff).

NGC 300 (Sculptor; Laustsen, Madsen, West, 1991)

5–7 Mpc: M101 group (“pinwheel galaxy”). Important because of high L.

Adam Block/NOAO/AURA/NSF

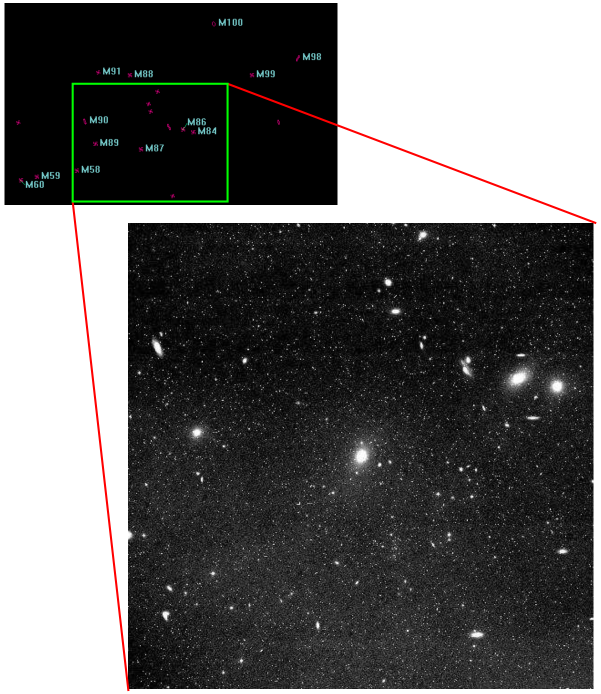

15–20 Mpc: Virgo cluster.

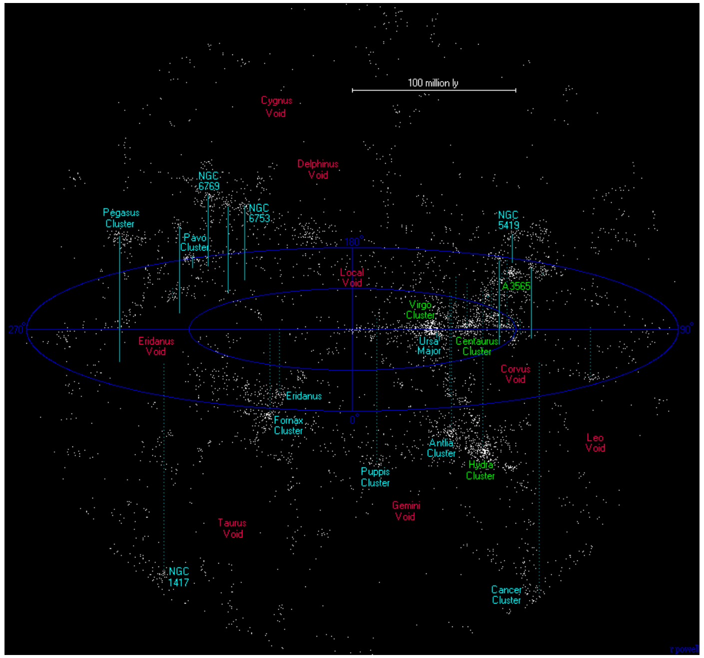

source: `http://www.atlasoftheuniverse.com/200mill.html`

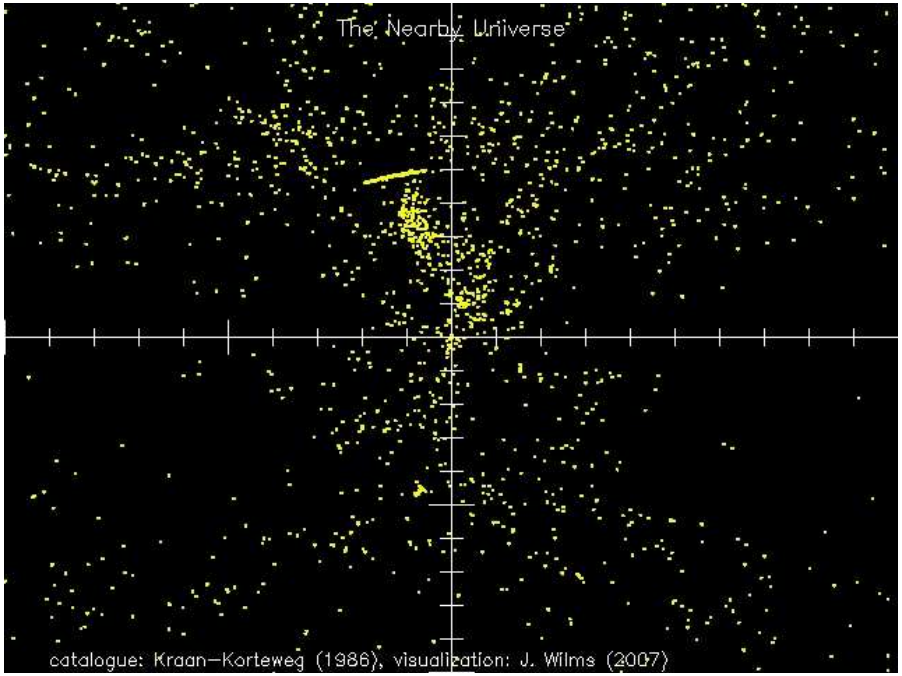

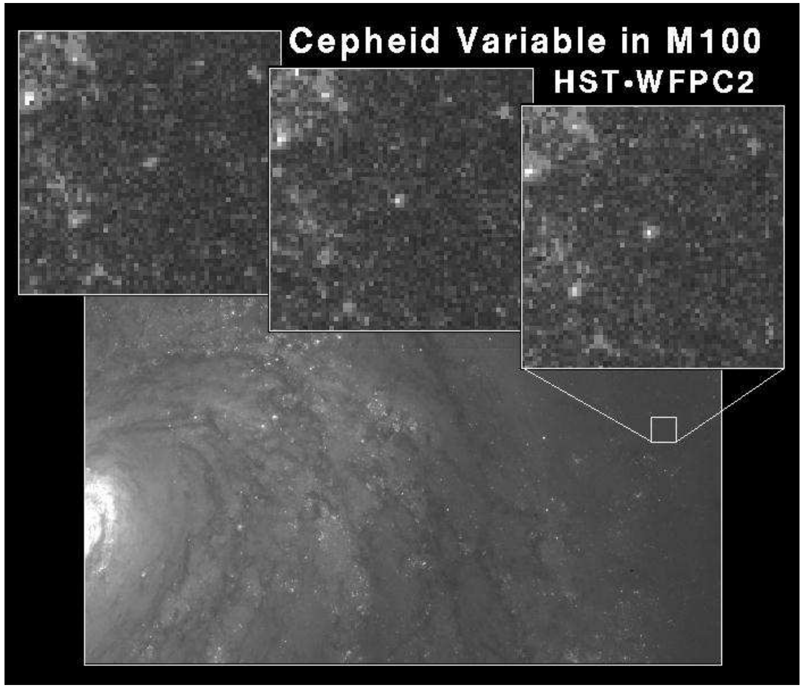

STScI PR94-49

Cepheids, III

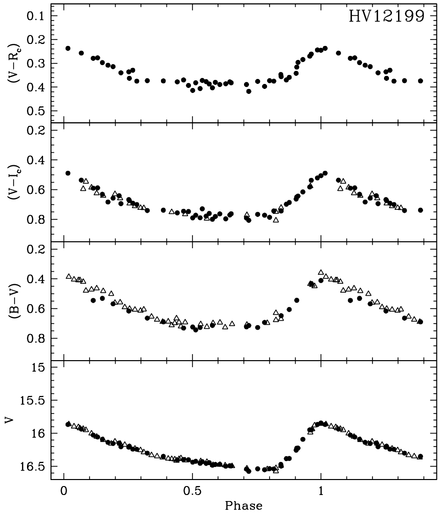

Cepheids:

- Luminous stars ($L \sim 1000\,L_\odot$) in instability strip (He II–He III ionization)
- large intensity amplitude variation,
- $P \sim 2\ldots150\,$d (easily measurable).

Review: Feast (1999).

(Gieren et al., 2000, Fig. 3)

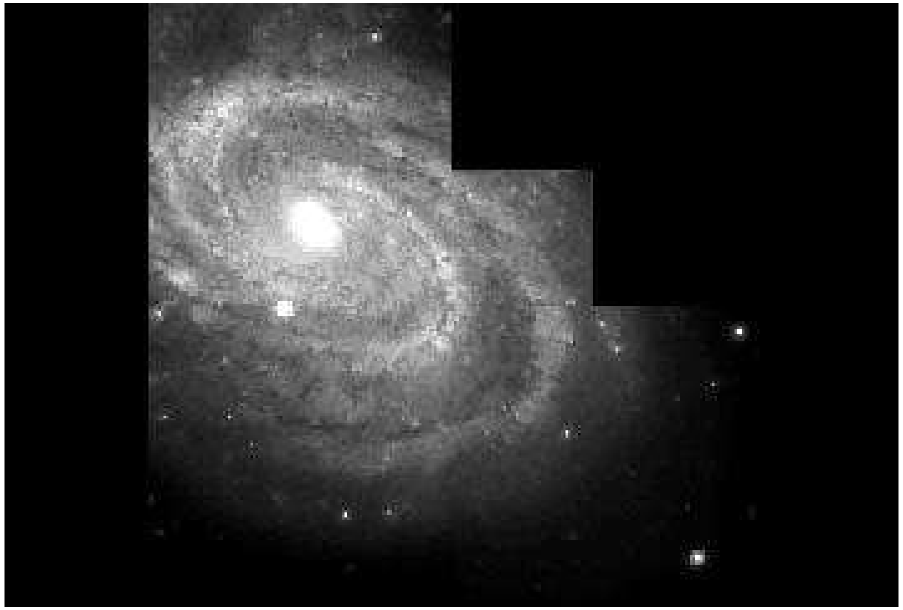

STScI

Cepheids, IV

© ASP

Henrietta Leavitt (1868–1921):

- Graduated from Radcliffe College
- from 1895: volunteer at Harvard Observatory
- was ill, and partially deaf as a result
- 1902: back at Harvard Obs
- discovered 1777 variable stars in LMC
- 1912: discovered Period-Luminosity relation of Cepheids in SMC, but was not allowed to follow up on this
- later: defined Harvard photographic magnitude system
- died of cancer in 1921

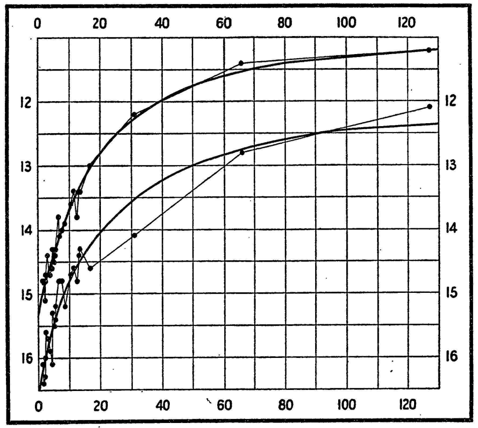

Fig. 1.

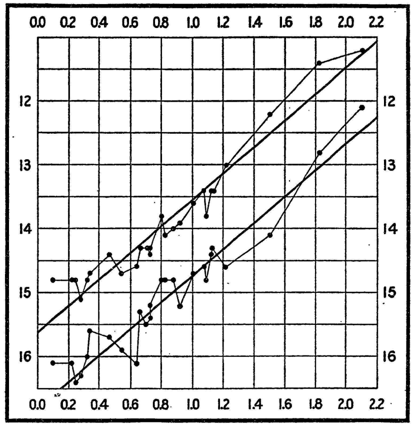

Fig. 2.

X-axis: period in days, Y-axis: magnitude

Leavitt & Pickering, 1912, Periods of 25 Variable Stars in the Small Magellanic Cloud, Harvard College Observatory Circular, vol. 173, pp. 1–3

Cepheids, VI

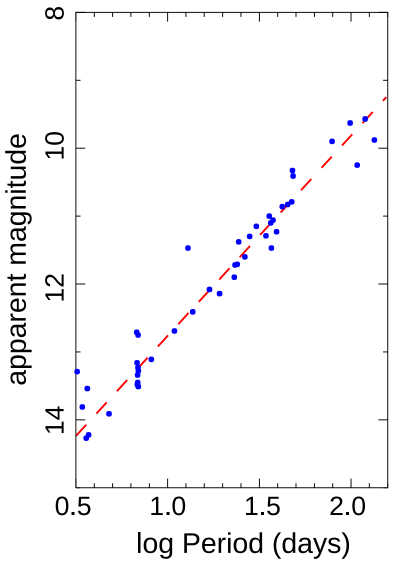

Period-Luminosity (PL) relation: $M_V \propto -2.76 \log P$.

Low luminosity Cepheids have lower periods.

There are indications that there is also an influence of the color

$\Longrightarrow$ Period-Luminosity-Color (PLC) relation

Note: W Vir stars, also called type II Cepheids = “little brother of Cepheids” (present in globular clusters). Less luminous than normal Cepheids, similar PLC relation, first confused with Cepheids $\Longrightarrow$ Cause for early thoughts of much smaller universe.

PL relation for the LMC Cepheids (after Mould, Kennicutt, Jr. & Freedman, 2000, Fig. 2).

Cepheids, VII

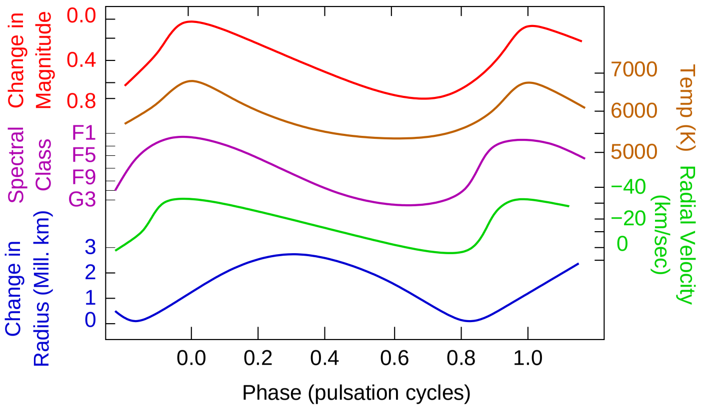

after `http://csep10.phys.utk.edu/astr162/lect/index.html`

Typical variation of measurable parameters over one pulsation.

Cepheids, VIII

Physics of Period-Luminosity-Color relation:

Star pulsates such that outer parts remain bound:

$$\frac{1}{2}\left(\frac{R}{P}\right)^2 \lesssim \frac{GM}{R} \quad \Longrightarrow \quad \frac{M}{R^3} \propto P^{-2} \tag{9.13}$$

where P period. Therefore:

$$P \propto \rho^{-1/2} \quad \Longleftrightarrow \quad P\rho^{1/2} = Q \tag{9.14}$$

(Q: pulsational constant, $\rho \propto MR^{-3}$ mean density). But Radius R related to luminosity L:

$$L = 4\pi R^2 \sigma T^4 \quad \Longrightarrow \quad R \propto L^{1/2} T^{-2} \tag{9.15}$$

Inserting everything into Eq. (9.14) gives:

$$PL^{-3}T^3 = \text{const.} \Longleftrightarrow \quad \log P - 3\log L + 3\log T = \text{const.} \tag{9.16}$$

But: *bolometric magnitude:* $M_{\text{bol}} \propto -\log L$, and *colors:* B − V $\propto \log T$ such that

$$c_1 \log P + c_2 M_{\text{bol}} + c_3(\text{B} - \text{V}) = \text{const.} \tag{9.17}$$

where $c_{1,2,3}$ calibration constants.

Cepheids, IX

Calibration: Need slope and zero point of PLC.

Slope: Observations of nearby galaxies (e.g., open clusters in LMC)

Zero point is difficult:

- Cepheids in galactic clusters, distance to these via ZAMS fitting
  $\Longrightarrow$ problematic due to age dependency of ZAMS.
- Hipparcos: geometrical distances
  $\Longrightarrow$ problematic due to low SNR (resulting in 9% systematic error.
- Baade-Wesselink using IR info (low metallicity dependence).

Typical relations (Mould et al., 2000, 32 Cepheids):

$$\begin{aligned} M_\mathrm{V} &= -2.76\log P - 1.40 + C(Z) \\ M_\mathrm{I} &= -3.06\log P - 1.81 + C(Z) \end{aligned} \tag{9.18}$$

The metallicity (color) dependence is roughly

$$(m-M)_\mathrm{true} = (m-M)_\mathrm{PL} - \gamma \log Z/Z_\mathrm{LMC} \tag{9.19}$$

where $\gamma = -0.11 \pm 0.03\,\mathrm{mag/dex}$ (Z: metallicity) (=Cepheids with larger Z are fainter).

Cepheids, X

Notes:

1. Is the pulsational constant a constant? (or is $Q = Q(\rho, P)$?):
   $\Longrightarrow$ possible deviation from PLC, especially at high luminosity
   $\Longrightarrow$ adds uncertainty at large distances.
2. M_V depends on metallicity
   $\Longrightarrow$ LMC Cepheids *are* bluer [$Z_\mathrm{LMC} < Z_\odot$]), but the exact value of γ in Eq. (9.19) is very uncertain.
   For V and I magnitudes, most probably $\delta(m-M)_0/\delta[\mathrm{O/H}] \lesssim -0.4\,\mathrm{mag\,dex^{-1}}$, however, others find $+0.75\,\mathrm{mag\,dex^{-1}}$, see Ferrarese et al. (2000) for details...
3. Stellar evolution unclear (multiple crossings of instability strip are possible).

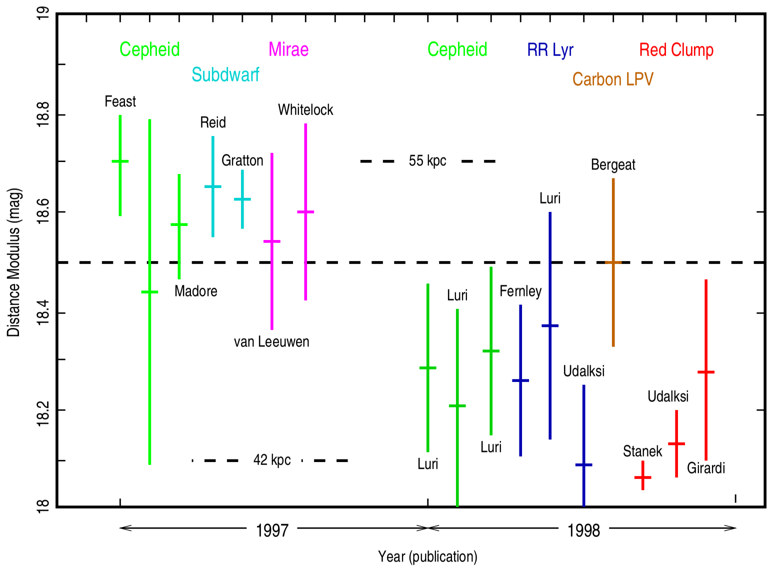

LMC distance: “anchor point” of extragalactic distance scale.

After Gaia Science Workgroup

Strong dependence on Hipparcos calibration.

DM ranges between 18.7 ± 0.1 mag (Feast & Catchpole) and 18.57 ± 0.11 mag (Madore & Freedman)

Currently, the distance to the LMC is less well known than desirable.

PN Luminosity Function, I

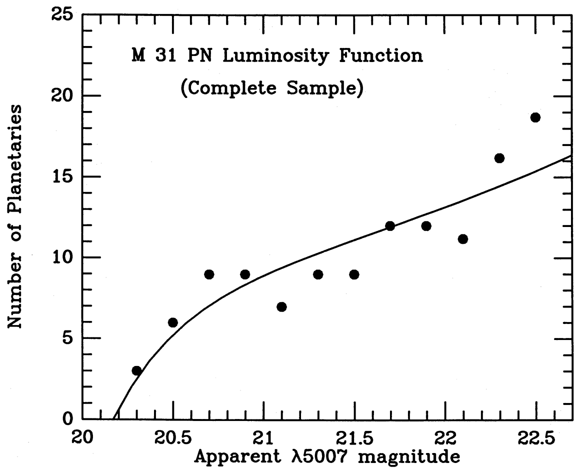

Planetary Nebulae have empirical universal luminosity function.

Measurement of “cutoff magnitude” M_PN
$\Longrightarrow$ Standard candle!

PN detection with narrow band filter of O[III]λ5007Å.

(Ciardullo et al., 1989, Fig. 4)

$$N(M) \propto \mathrm{e}^{0.307M}\left(1 - \mathrm{e}^{3(M_\mathrm{PN}-M)}\right) \tag{9.20}$$

PN Luminosity Function, II

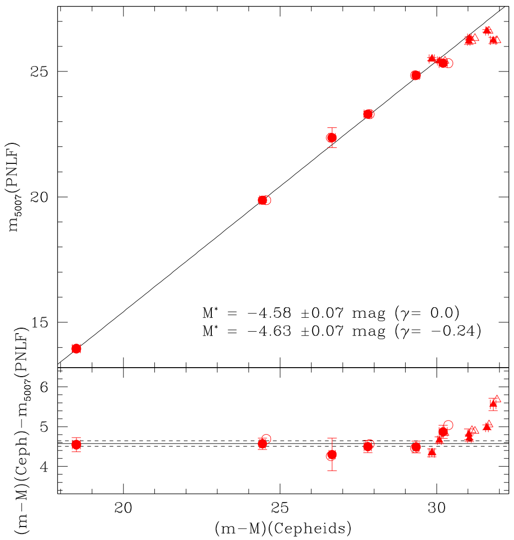

Result of calibration using Cepheid distances (Ferrarese et al., 2000):
Cutoff of luminosity function:

$$M_{\mathrm{PN}} = -4.58 \pm 0.13\,\mathrm{mag} \tag{9.21}$$

Works out to ∼40 Mpc with 8 m class telescope.

(Ferrarese et al., 2000, Fig. 3), left to right: LMC, M31, NGC 300, M81, M101, NGC 3368, and several galaxy groups.

PN Luminosity Function, III

Caveats: Effects of metallicity, population age, parent galaxy most probably small, but

- Contamination by H II regions (but distinguish using Hα/[O III] ratio.
- Background emission-line galaxies at $z = 3.1$
- intracluster PNe (i.e., PNe outside galaxies)

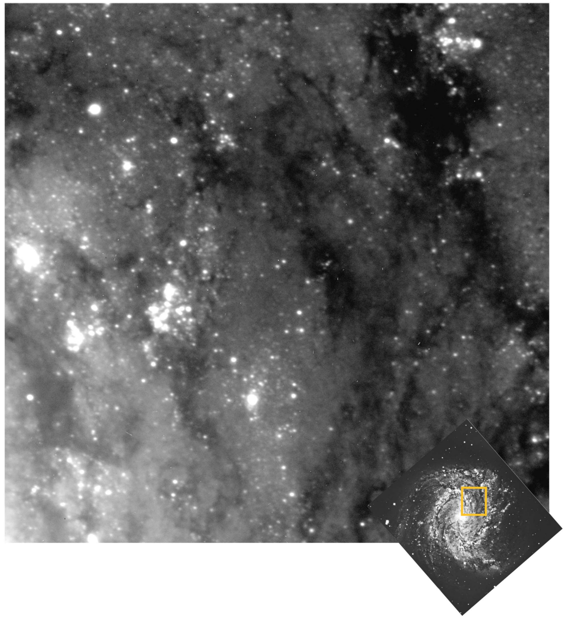

The VLT Looks Deep into a Spiral Galaxy

ESO PR Photo 20/98 (23 June 1998)

Brightest Stars, II

Brightest Stars= O, B, A supergiants, absolute magnitudes usable in local group, although there is a large scatter.

Reason: there is an upper limit to stellar luminosity due to mass loss in supergiants.

Possible Improvement: Strength of Balmer series lines. Hα and Hβ appear biased (class of supergiants with anomalously strong Balmer lines?).

Problems:

- Contamination by foreground halo stars
  $\Longrightarrow$ Choose stars with unusual color (rare, i.e. less foreground contamination): $\mathrm{B}-\mathrm{V} < 0.4$ or $\mathrm{B}-\mathrm{V} > 2.0 \Longrightarrow$ Tip of Red Giant Branch
- Internal extinction.
- Scatter in max. L
  $\Longrightarrow$ Average over brightest N stars (Sandage, Tammann: $N = 3$).
- Metallicity dependence.

Brightest Stars, III

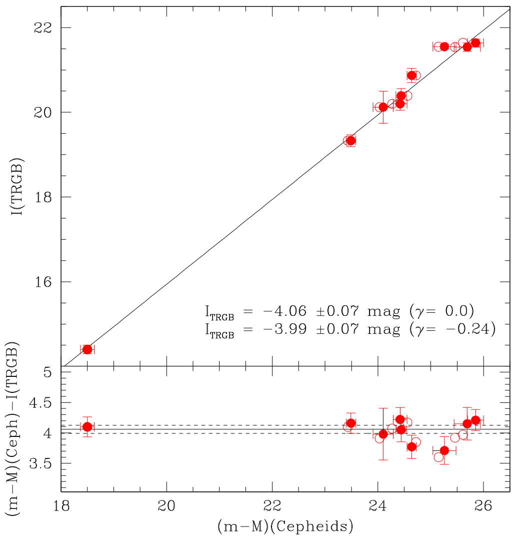

Tip of Red Giant Branch: Usable within local group, possibly out to Virgo.

Calibration:

$$M_\mathrm{I} = -4.06 \pm 0.13\,\mathrm{mag} \quad (9.22)$$

(Ferrarese et al., 2000, Fig. 1)

Globular Clusters

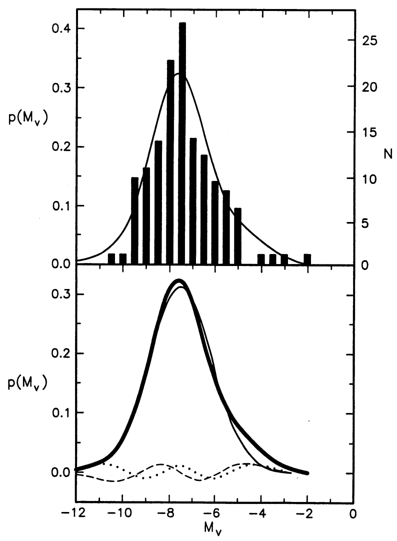

Globular Cluster Luminosity Function is ∼Gaussian
⟹ Use maximum of distribution (“turnover magnitude”, M_T) as standard candle.
From Virgo and Fornax Cepheid distances (Ferrarese et al., 2000):

$$M_\mathrm{T,\,V} = -7.60 \pm 0.25\,\mathrm{mag} \qquad (9.23)$$

Caveats:

1. M_T depends on luminosity and type of host galaxy (GC of dwarf galaxies weaker by ∼ 0.3 in V).
2. Metallicity of galaxy cluster influences M_T.
3. Measurement difficult (need the weak GCs!).
4. Large scatter in data ⟹ Method rather unreliable.

(MW GCs, Abraham & van den Bergh, 1995, Fig. 1)

Surface Brightness Fluctuations, I

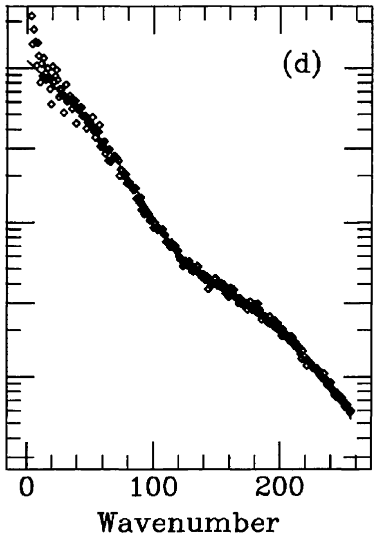

For early type galaxies: Assume N stars in picture element (pixel), with average flux f each.

$$\Longrightarrow \text{Mean pixel intensity:} \quad \mu = Nf \qquad (9.24)$$

independent of distance, since $N \propto r^2$ and $f \propto r^{-2}$.
Standard deviation between pixels (Poisson!):

$$\sigma = \sqrt{N} f \propto r^{-1} \qquad (9.25)$$

and therefore

$$f = \frac{\sigma^2}{\mu} = \frac{L}{4\pi r^2} \qquad (9.26)$$

which gives the distance r.

Review: Blakeslee, Ajhar & Tonry (1999).

Complication: Adjacent pixels not independent (point spread function of telescope!)
⟹ Use radial power spectrum to obtain σ^2 and μ.

(Ajhar et al., 1997, Fig. 3d)

Surface Brightness Fluctuations, II

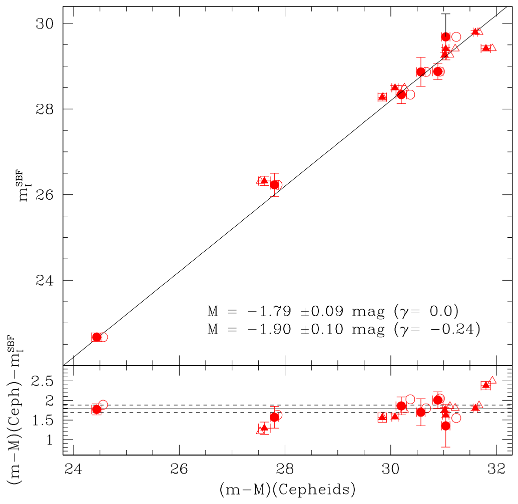

Luminosity of galaxy dominated by Red Giant Branch stars
⟹ Strong wavelength and color dependence
⟹ Primary calibration: I-band plus broad-band color dependency to give standard candle.
Often also used: HST WFPC2 plus F814W filter (close to I-band),

$$M_\mathrm{F814W} = (-1.70 \pm 0.16) + (4.5 \pm 0.3)\,[(\mathrm{V}-\mathrm{I})_0 - 1.15] \quad (9.27)$$

Works out to ∼ 70 Mpc with HST.
(Ferrarese et al., 2000, Fig. 5)

Novae, I

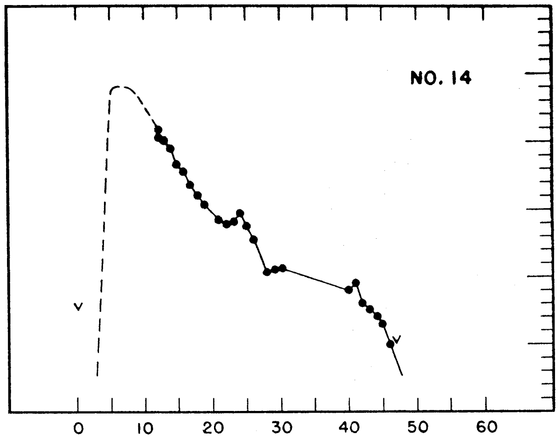

“classical nova”= explosion on surface of white dwarf

Novae only in binary systems

$\Longrightarrow$ slow accretion of material onto WD

$\Longrightarrow$ outer skin reaches M_{crit} for fusion

$\Longrightarrow$ explosion

$\Longrightarrow$ ejection of $10^{-6} \dots 10^{-4}\,M_\odot$ with $v \sim 500\,\text{km}\,\text{s}^{-1}$

Explosion produces characteristic lightcurve.

(Nova in M31, Arp, 1956, p. 18)

Novae, II

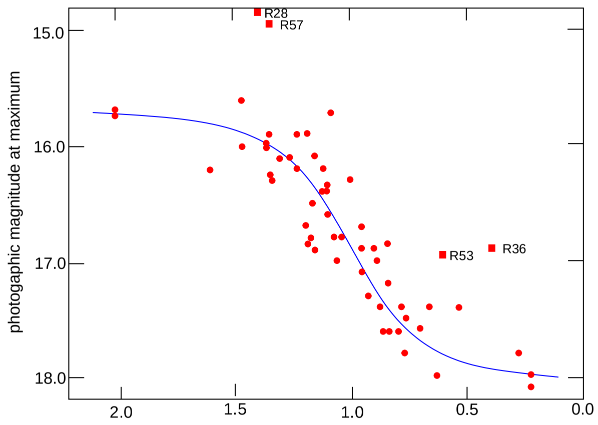

(after van den Bergh & Pritchet, 1986, Fig. 1).

Strong scatter in lightcurves (higher $L_{\max} \Longrightarrow$ faster decline, but typically $\sim$ 3× brighter than Cepheids), but good Correlation luminosity vs. decline timescale (t_i, time to reach $m(t_i) = m_{\max} + i$). *Calibration:* galactic novae.

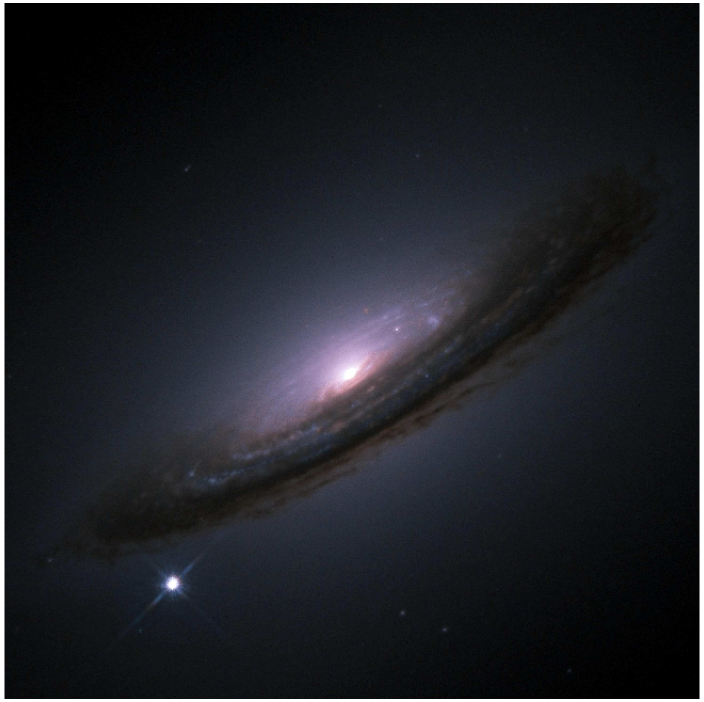

Supernovae have luminosities comparable to whole galaxies: $\sim 10^{51}\,\text{erg}\,\text{s}^{-1}$ in light, 100× more in neutrinos.

SN1994d (HST WFPC)

Type Ia Supernovae, II

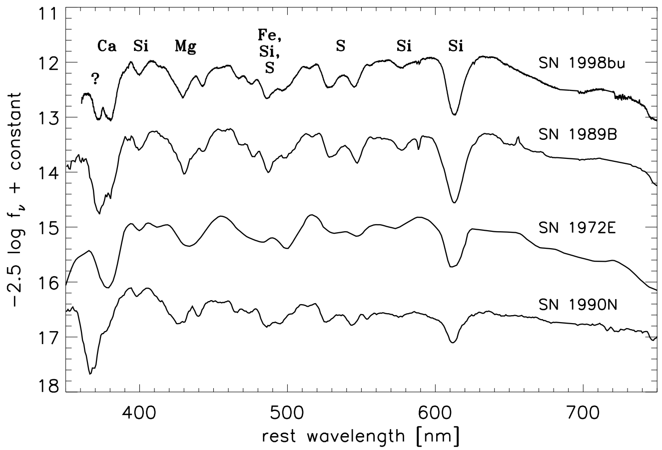

(Spectra of several SNe at maximum light Jha et al., 1999, Fig. 6)

Different supernovae can have very similar spectra.

$\Longrightarrow$ Allows their classification.

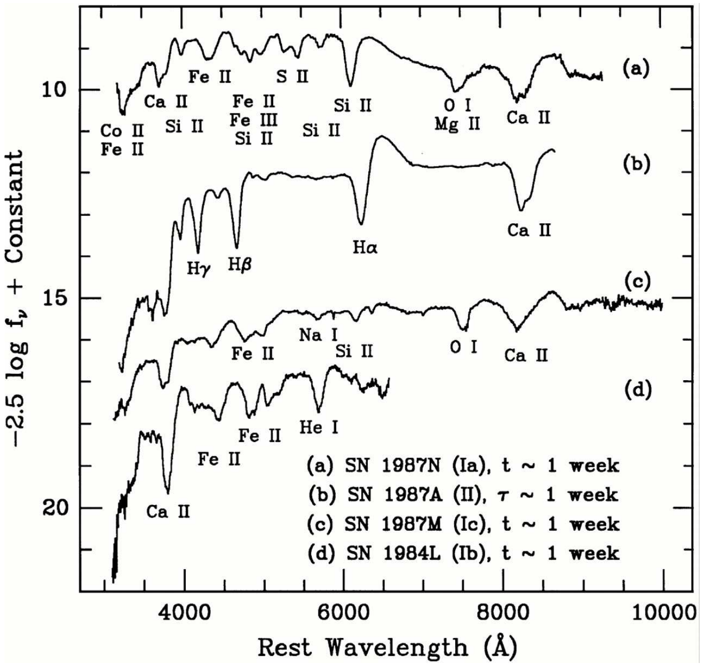

(Filippenko, 1997, Fig. 1); t: time after maximum light; τ: time after explosion; P Cyg profiles give $v \sim 10000\,\mathrm{km\,s^{-1}}$

Rough classification (Minkowski, 1941):

Type I: no hydrogen in spectra; subtypes Ia, Ib, Ic

Type II: hydrogen present, subtypes II-L, II-P

Note: pre 1985 subtypes Ia, Ib had different definition than today ⟹ beware when reading older texts.

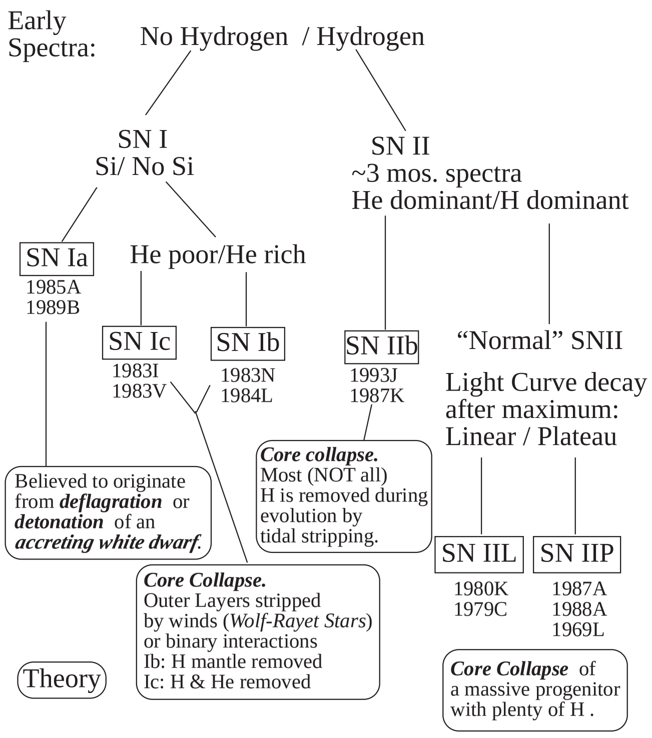

Early Spectra:

No Hydrogen / Hydrogen

SN I
Si/ No Si

SN II
~3 mos. spectra
He dominant/H dominant

SN Ia
1985A
1989B

He poor/He rich

SN Ic
1983I
1983V

SN Ib
1983N
1984L

SN IIb
1993J
1987K

“Normal” SNII

Light Curve decay
after maximum:
Linear / Plateau

SN IIL
1980K
1979C

SN IIP
1987A
1988A
1969L

Believed to originate from ***deflagration*** or ***detonation*** of an ***accreting white dwarf.***

Core collapse.
Most (NOT all)
H is removed during
evolution by
tidal stripping.

Core Collapse.
Outer Layers stripped
by winds (*Wolf-Rayet Stars*)
or binary interactions
Ib: H mantle removed
Ic: H & He removed

Core Collapse of
a massive progenitor
with plenty of H .

Theory

courtesy M.J. Montes

Type Ia Supernovae, V

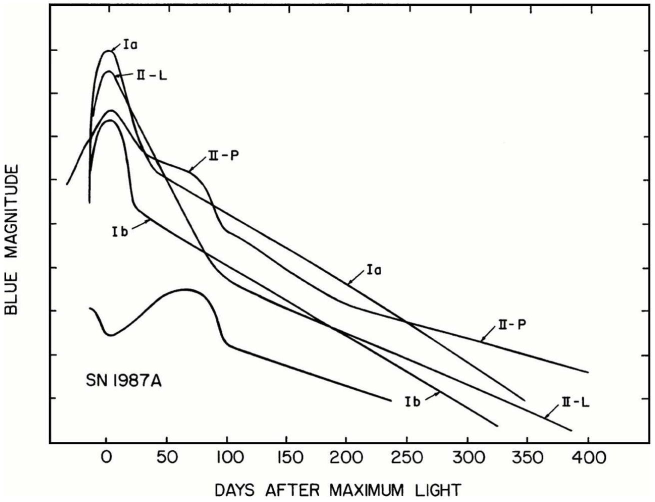

(Filippenko, 1997, Fig. 3)

Light curves of SNe I all very similar, SNe II have much more scatter.

SNe II-L (“linear”) resemble SNe I

SNe II-P (“plateau”) have const. brightness to within 1 mag for extended period of time.

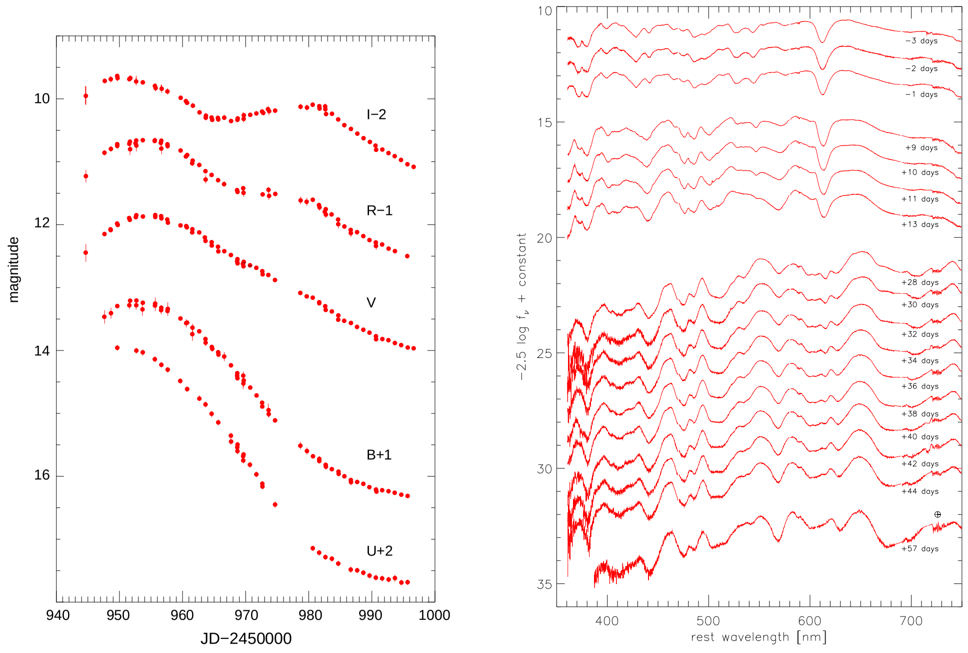

(SN 1998bu in M96, Jha et al., 1999, Figs. 2 and 4)

Type Ia Supernovae, VII

Clue on origin from supernova statistics:

- SNe II, Ib, Ic: never seen in ellipticals; rarely in S0; generally associated with spiral arms and H II regions.

$\Longrightarrow$ *progenitor of SNe II, Ib, Ic:* massive stars ($\gtrsim 8\,M_\odot$) $\Longrightarrow$ core collapse

- SNe Ia: all types of galaxies, no preference for arms, almost no scatter in lightcurves

$\Longrightarrow$ *progenitor of SNe Ia:* accreting carbon-oxygen white dwarfs, undergoing thermonuclear runaway

Rule of thumb: 1. . . 3 SNe per galaxy and per century

Type Ia Supernovae, VIII

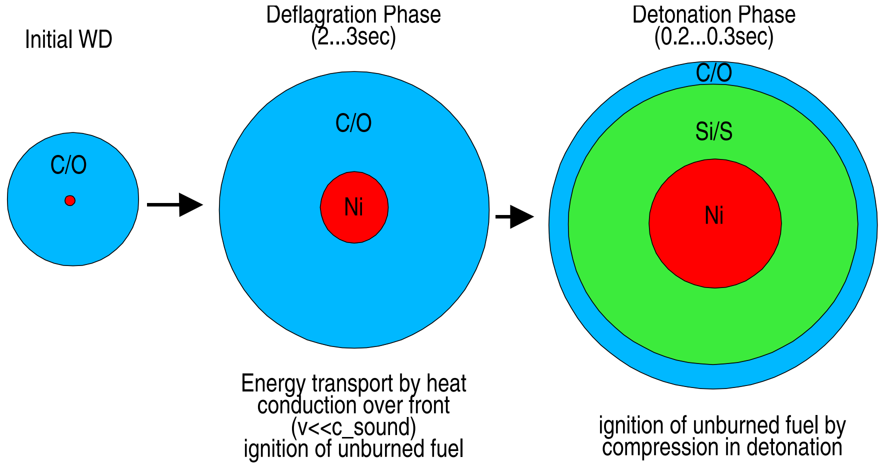

Initial WD

Deflagration Phase
(2...3sec)

Energy transport by heat
conduction over front
(v<<c_sound)
ignition of unburned fuel

Detonation Phase
(0.2...0.3sec)

ignition of unburned fuel by
compression in detonation

after P. Höflich

Type Ia Supernovae, IX

SN Ia = Explosion of CO white dwarf when pushed over Chandrasekhar limit (1.4 $M_\odot$) (via accretion?).

$\Longrightarrow$ Always similar process

$\Longrightarrow$ Very characteristic light curve: fast rise, rapid fall, exponential decay ("FRED") with half-time of 60 d.

60 d time scale from radioactive decay $\text{Ni}^{56} \rightarrow \text{Co}^{56} \rightarrow \text{Fe}^{56}$ ("self calibration" of lightcurve if same amount of Ni^{56} produced everywhere).

Calibration: SNe Ia in nearby galaxies where Cepheid distances known.

At maximum light:

$$M_\text{B} = -18.33 \pm 0.11 + 5 \log h_{100} \quad (L \sim 10^{9\ldots10}\,L_\odot) \tag{9.28}$$

Intrinsic dispersion: $\lesssim$0.25 mag (possibly due to size of clusters analyzed?!?)

Observable out to 1000 Mpc

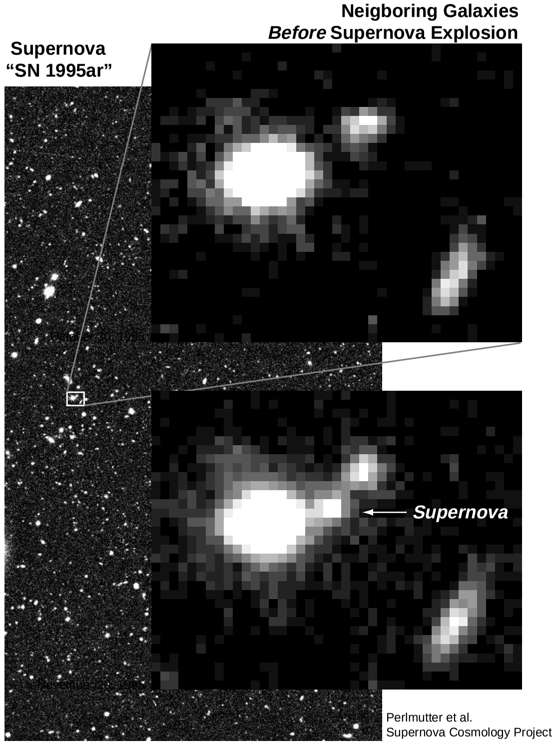

Perlmutter et al.
Supernova Cosmology Project

Type Ia Supernovae, XI

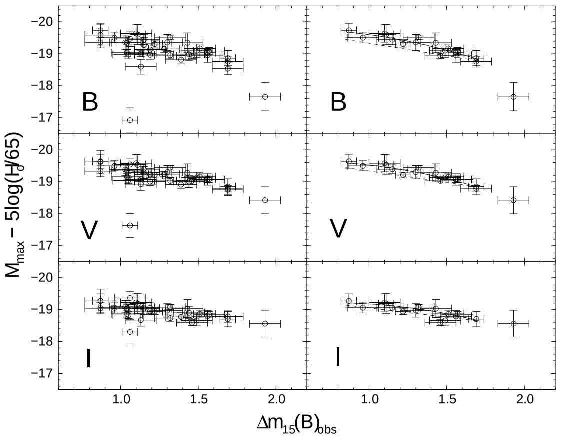

(Phillips et al., 1999, Fig. 8)

Caveats:

1. Are they *really* identical?
   $\Longrightarrow$ history of pre-WD star?
2. Correction for extinction in parent galaxy difficult.
3. Baade-Wesselink for calibration Eq. (9.28) depends crucially on assumed $(\mathrm{B}-\mathrm{V})$-T_{eff} relation.
4. Some SN Iae spectroscopically peculiar $\Longrightarrow$ Do not use these!
5. Decline rate and color vary, but max. brightness and decline rate correlate (see figure).

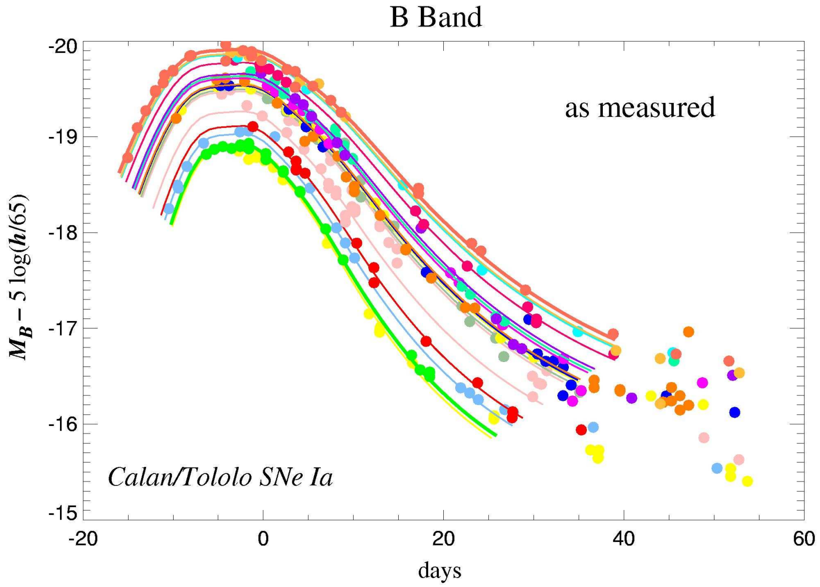

Lightcurves of Hamuy et al. SN Ia sample (18 SNe discovered within 5 d past maximum, with $3.6 < \log cz < 4.5$, i.e., $z < 0.1$)

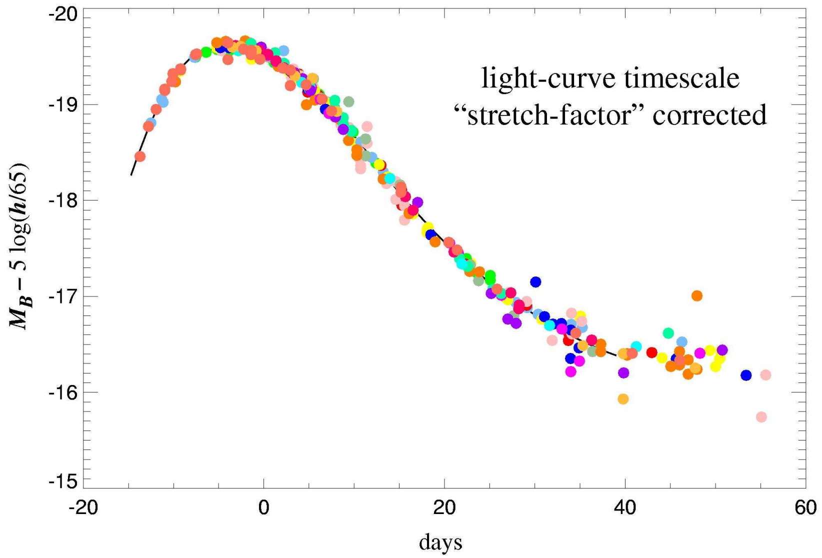

Kim, *et al.* (1997)

Lightcurves of Hamuy et al. SN Ia sample (18 SNe discovered within 5 d past maximum, with $3.6 < \log cz < 4.5$, i.e., $z < 0.1$), after correction of systematic effects and time dilatation (Kim et al., 1997).

Type Ia Supernovae, XIV

Recalibration of SN Ia distances with Cepheids gives (Gibson et al., 2000):

$$\log H_0 = 0.2\Big\{M_{\mathrm{B}}^{\mathrm{max}} - 0.720(\pm 0.459) \cdot [\Delta m_{\mathrm{B},15,t} - 1.1] - 1.010(\pm 0.934) \cdot [\Delta m_{\mathrm{B},15,t} - 1.1]^2 + 28.653(\pm 0.042)\Big\} \quad (9.29)$$

where

$$\Delta m_{\mathrm{B},15,t} = \Delta m_{\mathrm{B},15} + 0.1E(\mathrm{B}-\mathrm{V}) \quad (9.30)$$

where

$\Delta m_{\mathrm{B},15}$: observed 15 d decline rate,
$E(\mathrm{B}-\mathrm{V})$: total extinction (galactic+intrinsic).

Eq. (9.29) valid for B-band, equivalent formulae exist for V and I.

Overall, the calibration is good to better than 0.2 mag in B.

Tully-Fisher, I

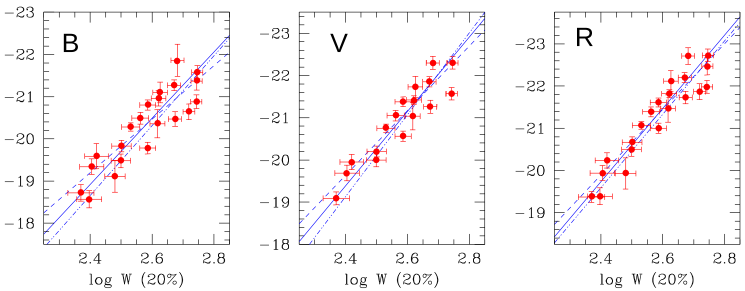

(after Sakai et al., 2000, Fig. 1)

Tully-Fisher relation for spiral galaxies: Width of 21 cm line of H correlated with galaxy luminosity:

$$M = -a \log\left(\frac{W_{20}}{\sin i}\right) - b \tag{9.31}$$

where W_{20}: 20% line width (km s^{-1}; typically $W_{20} \sim 300\,\mathrm{km\,s^{-1}}$), i inclination angle.

For the B- and I-Bands (Sakai et al., 2000):

	B	I
a	7.97± 0.72	9.24± 0.75
b	19.80± 0.11	21.12± 0.12

Tully-Fisher, II

Qualitative Physics: Line width related to mass of galaxy: $W/2 \sim V_{\max}$, where $V_{\max}$ max. velocity of rotation curve

$\Longrightarrow$ Assume $M/L =$ const. (good assumption)

$\Longrightarrow$ width related to luminosity.

Detailed physical basis unknown. Might be related to galaxy formation ("hierarchical clustering", see later).

I-band is better (less internal extinction).

Caveats:

1. Determination of inclination i.
2. Influence of turbulent motion within galaxy.
3. Constants dependent on galaxy type (Sa and Sb similar, Sc more luminous by factor of ∼2).
4. Optical extinction.
5. Intrinsic dispersion ∼0.2 mag.
6. Barred Galaxies problematic.

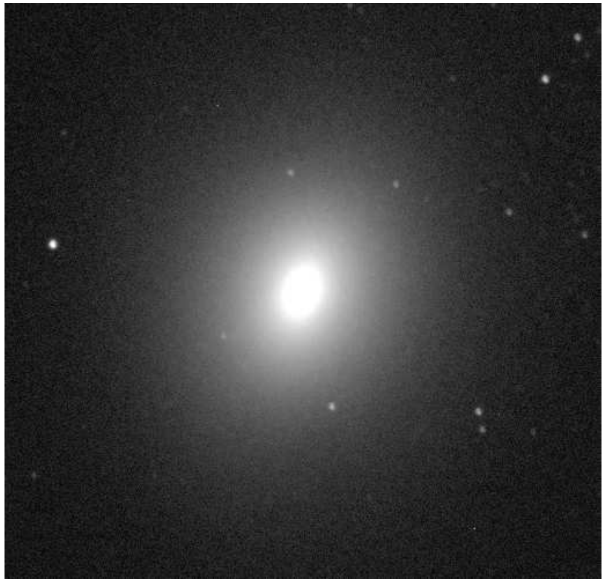

M32 (companion of Andromeda), courtesy W. Keel

"Faber-Jackson" law for elliptical galaxies:

The luminosity L of an elliptical galaxy scales with its intrinsic velocity dispersion, σ, as $L \propto \sigma^4$.

Note that ellipticals have virtually no Hydrogen

$\Longrightarrow$ cannot use 21 cm.

Ellipticals: $$M_\mathrm{B} = -19.38 \pm 0.07 - (9.0 \pm 0.7)(\log\sigma - 2.3) \tag{9.32}$$

Lenticulars (Type S0): $$M_\mathrm{B} = -19.65 \pm 0.08 - (8.4 \pm 0.8)(\log\sigma - 2.3) \tag{9.33}$$

D_n-σ

The Faber-Jackson law is a specialized case of the more general D_n–σ-relation:

The intensity profile of an elliptical galaxy is given by de Vaucouleurs' $r^{1/4}$ law:

$$I(r) = I_0 \exp\left(-(r/r_0)^{1/4}\right) \quad \Longrightarrow \quad L = \int I \propto I_0 r_0^2 \tag{9.34}$$

Because of the virial theorem ($E_\mathrm{kin} = -E_\mathrm{pot}/2$):

$$\frac{1}{2} m\sigma^2 = G\frac{mM}{r_0} \quad \Longleftrightarrow \quad \sigma^2 \propto \frac{M}{r_0} \tag{9.35}$$

where σ: velocity dispersion.

Assume a mass-to-light ratio

$$M/L \propto M^\alpha \tag{9.36}$$

($\alpha \sim 0.25$). and use r_0 from Eq. (9.34) to obtain

$$L^{1+\alpha} \propto \sigma^{4-4\alpha} I_0^{\alpha-1} \tag{9.37}$$

This is called the "fundamental plane" relationship (Dressler et al., 1987).

D_n-σ

Observational version of the fundamental plane relationship: Instead of inserting r_0 and I_0, measure diameter D_n of aperture to reach some mean surface brightness (typically sky brightness, 20.75 mag arcsec^{-2} in B), and use calibration.

Note: Assumptions are

1. M/L same everywhere.
2. ellipticals have same stellar population everywhere

Calibration paper: Kelson et al. (2000).

Path to H_0

To obtain H_0, we need distances, and redshifts.

Redshifts: Trivial

Distances: Hubble Space Telescope Key Project on Extragalactic Distance Scale.

Summary paper: Freedman et al. (2001), there are a total of 29 papers on the HST key project!

Strategy:

1. Use high-quality candles: Cepheid variables as primary distance calibrator.
2. Calibrate secondary calibrators that work out to $cz = 10000\,\mathrm{km\,s^{-1}}$:
   - Tully-Fisher,
   - Type Ia Supernovae,
   - Surface Brightness Fluctuations,
   - Fundamental-plane for Ellipticals.
3. Combine uncertainties from these methods.

Velocity Field, I

Before determining H_0: correct for influence of velocity field (cluster motion with respect to comoving coordinates).

The observed redshift is given by

$$1 + z = (1 + z_{\mathrm{R}})\left(1 - \frac{v_0}{c} + \frac{v_{\mathrm{G}}}{c}\right) \qquad (9.38)$$

where

v_0: observer's radial velocity in direction of galaxy

v_{G}: radial velocity of the galaxy, difficult to find

z_{R}: cosmological redshift

Older galaxy catalogues often attempt to correct the measured values of z to produce “corrected redshifts”, e.g., by setting $v_{\mathrm{G}} = 0$ and

$$1 + z = (1 + z_{\mathrm{R}})\left(1 + \frac{v_0}{c}\right) \sim 1 + z_{\mathrm{R}} - \frac{v_0}{c} \quad\Longrightarrow\quad z_{\mathrm{R}} \sim z + \frac{v_0}{c} \qquad (9.39)$$

since v_0 was not well known before COBE $\Longrightarrow$ introduces unnecessary problems

$\Longrightarrow$ correction not used in recent redshift surveys! (see Harrison & Noonan, 1979, for details)

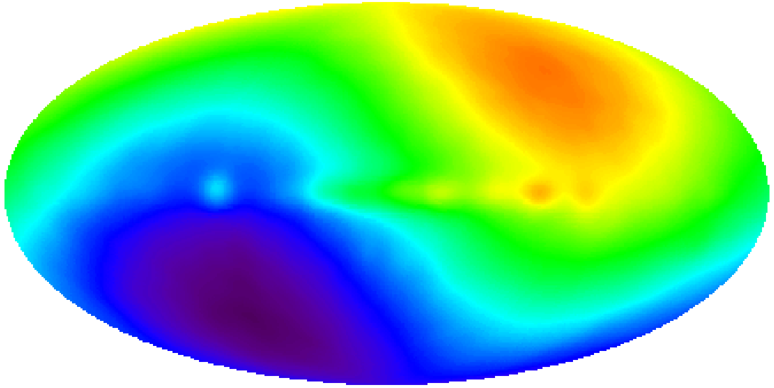

(COBE DMR; Bennett et al., 1996)

v_0 is easy to find $\Longrightarrow$ Measure velocity of Earth with respect to 3 K radiation. COBE finds $\Delta T = 3.353 \pm 0.024$ mK of 3K black-body spectrum of $T = 2.725 \pm 0.020$ K, using $\Delta T/T = v/c$.

$$v_0 = (369.1 \pm 2.6)\,\mathrm{km\,s^{-1}} \cdot \cos\theta_{\mathrm{CMB}} \qquad (9.40)$$

where $\theta_{\mathrm{CMB}} = \angle(\boldsymbol{v}, \boldsymbol{v}_{\mathrm{CMB}})$, and $\boldsymbol{v}_{\mathrm{CMR}}$ points towards

$$(l, b) = (264^{\circ}\!.26 \pm 0^{\circ}\!.33, 48^{\circ}\!.22 \pm 0^{\circ}\!.13)$$

$$(\alpha, \delta)_{\mathrm{J2000.0}} = (11^{\mathrm{h}}12^{\mathrm{m}}\!.2 \pm 0^{\mathrm{m}}\!.8, -7^{\circ}\!.06 \pm 0^{\circ}\!.16)$$

in constellation Crater.

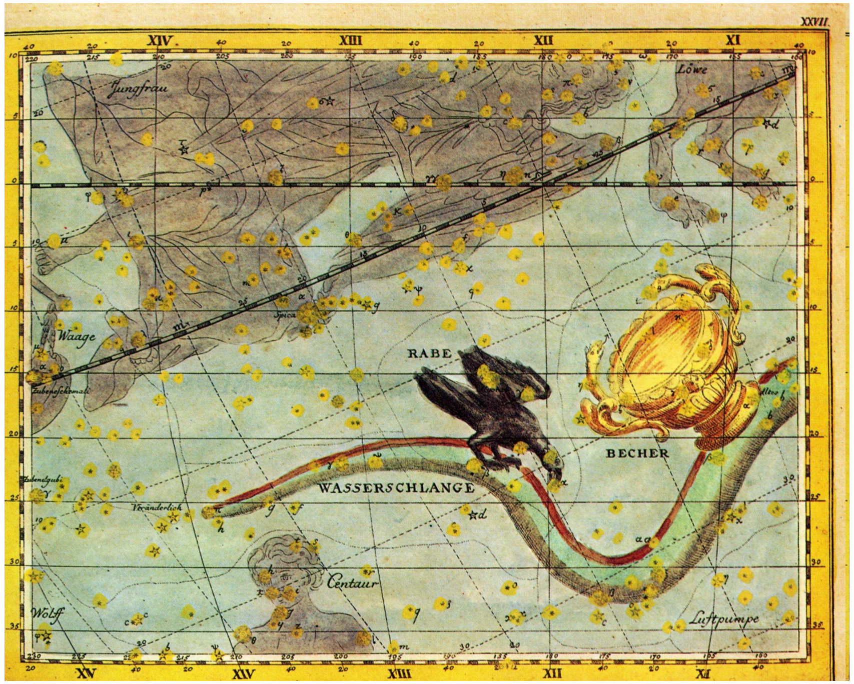

The constellation Crater ("Becher") in Johan Elert Bode's Sternatlas
(after Slawik/Reichert, Atlas der Sternbilder, Spektrum, 2004)

Velocity Field, IV

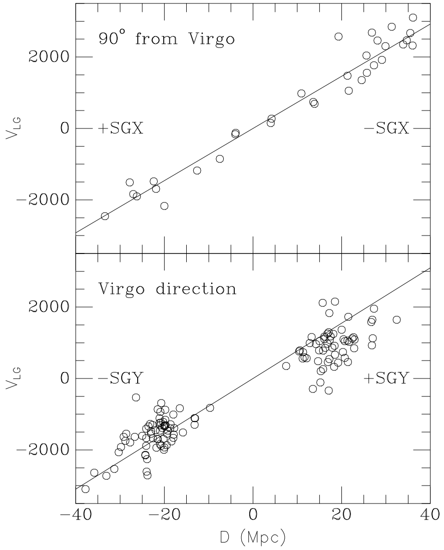

To get feeling for v_G out to Virgo, need to study local velocity field surrounding local group and beyond.

Two major velocity components:

1. Virgocentric infall (known since mid-1970s)
2. Motion towards great attractor ("Seven Samurai", 1980)

plus virialized galaxy motions within clusters.

General analysis: build maximum likelihood model of velocity field including above components *plus* Hubble flow. See Tonry et al. (2000) for details.

Galaxy moves within local group with $v \sim 630\,\mathrm{km\,s^{-1}}$

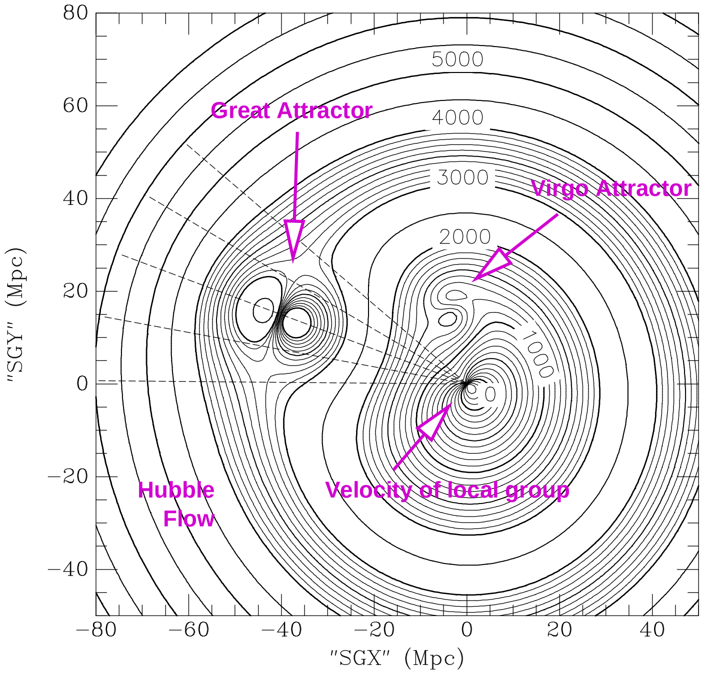

Decomposition of velocity field: (Mould et al., 2000, Tab. A1, note that Tonry et al. 2000 find slightly different values):

	$\alpha_{1950.0}$	$\delta_{1950.0}$
Virgo	12^h28^m	$+12^\circ 40'$
GA	13^h20^m	$+44^\circ 00'$
Shapley	13^h30^m	$+31^\circ 00'$

(v wrt. center of local group; *not* taking Hubble flow into account!).

(Tonry et al., 2000, Fig. 20)

H from HST

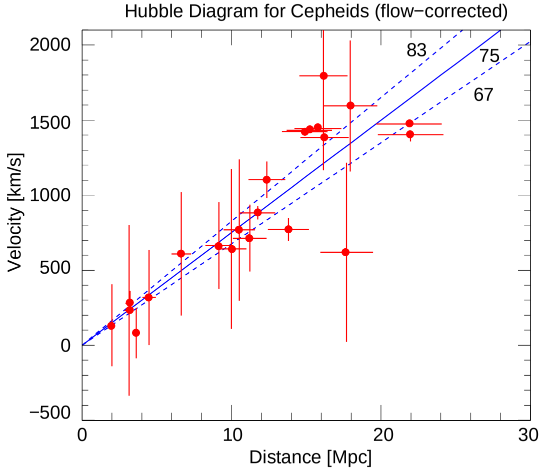

Freedman et al. (2001, Fig. 1)

To obtain H_0:

1. Determine d with Cepheids and HST
2. Determine "v", corrected for local velocity field
3. Draw Hubble-diagram
4. Regression Analysis $\Longrightarrow$ H_0

Value from HST Key Project:

$$H_0 = 75 \pm 10\,\mathrm{km\,s^{-1}\,Mpc^{-1}} \tag{9.41}$$

H from HST

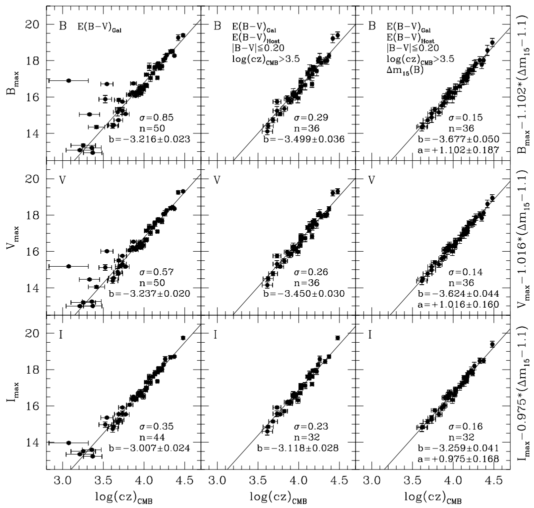

Cepheids alone: nearby

$\Longrightarrow$ systematic uncertainties due to local flow correction and small overall v

$\Longrightarrow$ use secondary candles to get to larger distances.

Example: magnitude-redshift diagram, analoguous to Hubble diagram ($m \propto -5\log I$, and $I \propto 1/r^2 \propto 1/z^2$ because of Hubble $\Longrightarrow m \propto \log cz$).

(SN Ia Hubble relations; left: full sample, middle: excluding strongly reddened SN Iae, right: same as middle, correcting for light-curve shape Freedman et al., 2001, Fig. 2)

H from HST

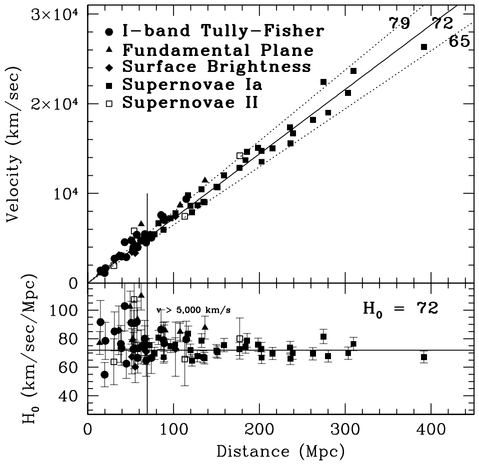

Freedman et al. (2001, Fig. 4)

Combining all secondary methods, best value found:

$$H_0 = 72 \pm 8\,\mathrm{km\,s^{-1}\,Mpc^{-1}} \tag{9.42}$$

H from HST

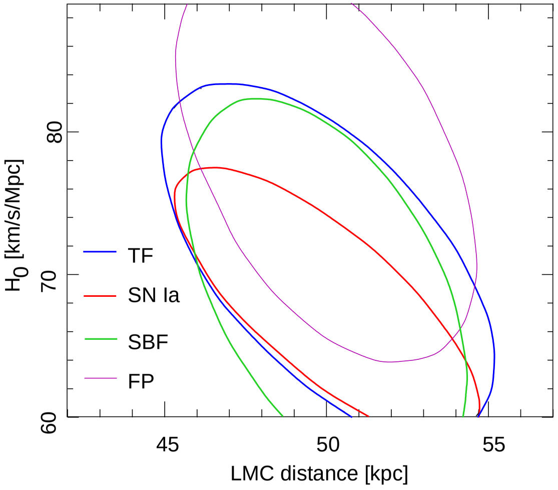

(after Mould et al., 2000, Fig. 5)

Major systematic uncertainty in current H_0 value: zero-point of Cepheid scale, i.e., distance to Large Magellanic Cloud.

Despite these problems:

$\Longrightarrow$ All current values approach $\sim$70 km s^{-1} Mpc^{-1}, with uncertainty $\sim$10%

H_0 controversy is over

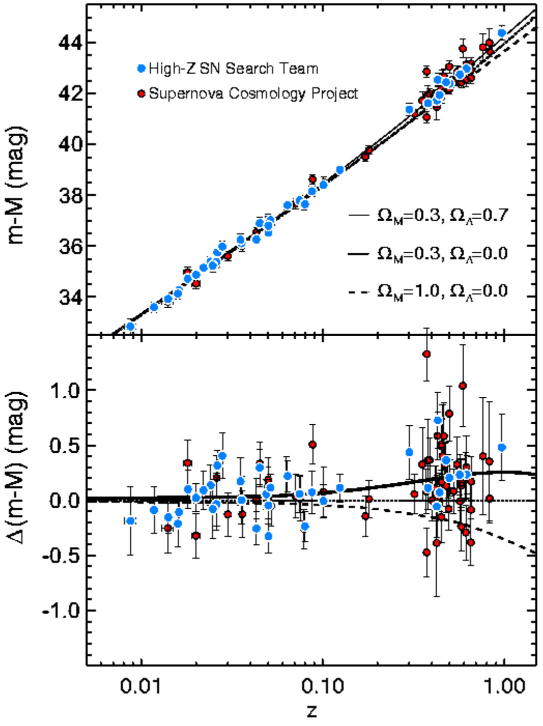

For larger distances: There are deviations from Hubble-Relation! Before we understand why: Need to understand the Big-Bang itself!

Abraham, R. G., & van den Bergh, S., 1995, ApJ, 438, 218

Ajhar, E. A., Lauer, T. R., Tonry, J. L., Blakeslee, J. P., Dressler, A., Holtzman, J. A., & Postman, M., 1997, Astron. J., 114, 626

Arp, H. C., 1956, Astron. J., 61, 15

Bennett, C. L., et al., 1996, ApJ, 464, L1

Blakeslee, J., Ajhar, E. A., & Tonry, J. L., 1999, in Post-Hipparcos Cosmic Candles, ed. A. H. . F. Caputo, (Dordrecht: Kluwer), 181, astro-ph/9807124

Ciardullo, R., Jacoby, G. H., Ford, H. C., & Neill, J. D., 1989, ApJ, 339, 53

Feast, M., 1999, PASP, 111, 775

Fenkart, R. F., & Binggeli, B., 1979, ApJS, 35, 271

Ferrarese, L., et al., 2000, ApJ, 529, 745

Filippenko, A. V., 1997, ARA&A, 35, 309

Freedman, W. L., et al., 2001, ApJ, 553, 47

Gibson, B. K., et al., 2000, ApJ, 529, 723

Gieren, W. P., Gómez, M., Storm, J., Moffett, T. J., Infante, L., Barnes, III, T. G., Geisler, D., & Fouqué, P., 2000, ApJS, 129, 111

Hanson, R. B., 1980, in Star Formation, ed. J. E. Hesser, Vol. 85, 71

Harrison, E. R., & Noonan, T. W., 1979, ApJ, 232, 18

Jacoby, G. H., et al., 1992, PASP, 104, 599

Jha, S., et al., 1999, Astrophys. J., Suppl. Ser., 125, 73

Kelson, D. D., et al., 2000, ApJ, 529, 768

Kim, A. G., et al., 1997, ApJ, 476, L63

Lee, J.-W., & Carney, B. W., 1999, ApJ, 117, 2868

Mould, J., Kennicutt, Jr., R. C., & Freedman, W., 2000, Rep. Prog. Phys., 63, 763

Mould, J. R., et al., 2000, ApJ, 529, 786

Phillips, M. M., Lira, P., Suntzeff, N. B., Schommer, R. A., Hamuy, M., & Maza, J., 1999, Astron. J., 118, 1766

Rowan-Robinson, M., 1985, The Cosmological Distance Ladder, (New York: Freeman)

Sakai, S., et al., 2000, ApJ, 529, 698

Seidelmann, P. K., (eds.) 1992, Explanatory Supplement to the Astronomical Almanac, (Mill Valley, CA: University Science Books)

Straniero, O., Chieffi, A., & Limongi, M., 1997, ApJ, 490, 425

Tonry, J. L., Blakeslee, J. P., Ajhar, E. A., & Dressler, A., 2000, ApJ, 530, 625

van den Bergh, S., & Pritchet, C. J., 1986, PASP, 98, 110

van Leeuwen, F., 2007, A&A, 474, 653